

Ruthenium-Biotin Conjugates

Conjugating Biotin to Ruthenium(II) Arene Units via Phosphine Ligand Functionalization

Lorenzo Biancalana,^[a] Martyna Gruchała,^[b] Lucinda K. Batchelor,^[c] Andrzej Błaż, ^[b]
Andrea Monti,^[a] Guido Pampaloni,^[a] Błażej Rychlik,^[b] Paul J. Dyson,^[c] and
Fabio Marchetti*^[a]

Abstract: Two-step functionalization of 4-diphenylphosphino benzoic acid with biotin afforded 2-(biotinyloxy)ethyl 4-(diphenylphosphanyl)benzoate (**LP**), that was subsequently used to synthesize the Ru(II) arene complexes [RuCl₂(η⁶-*p*-cymene)(**LP**)] (**1**), [Ru(C₂O₄)(η⁶-*p*-cymene)(**LP**)] (**2**) and [Ru(curc)(η⁶-*p*-cymene)(**LP**)]NO₃ (**3**)NO₃, the latter incorporating curcumin (**curcH**) as an additional bioactive fragment. [Ru(curc)(η⁶-*p*-cymene)(PPh₃)]NO₃ (**4**)NO₃ was also prepared as a reference compound. Compounds **2** and **3**)NO₃ exhibited excellent sta-

bility in water/DMSO solution while being slowly activated in the cell culture medium over 72 hours. Together with **LP**, they were therefore assessed for their antiproliferative activity towards a panel of cancer cell lines, with different levels of biotin transporter expression. The apparent affinity of the compounds towards avidin varies, and their antiproliferative activity does not correlate with biotin transporter expression, although it is systematically enhanced when biotin-free cell culture medium is used.

Introduction

The development of metal-based anticancer drugs that overcome the limitations of platinum compounds currently used in chemotherapy continues to receive considerable attention.^[1] In this respect, ruthenium compounds have emerged as promising alternatives, with [indazoleH][*trans*-Ru(*N*-indazole)₂Cl₄] (KP1019) and [imidazoleH][*trans*-Ru(*N*-imidazole)(*S*-DMSO)Cl₄] (NAMI-A), having undergone clinical evaluation.^[2] These Ru(III) compounds exhibit lower toxicities and side-effects than the clinically approved Pt(II) drugs, attributed to in situ reduction and activation of Ru(III) to Ru(II) species in the tumour environment.^{2,3} However, a key limitation of all of these drugs is that they do not efficiently target tumours. Consequently, efforts have been devoted to attaching targeting groups to metal-based drugs to enhance their uptake into cancer cells, by exploiting the different characteristics of cancerous and normal cells.^[4] Therefore, various small molecule targeting groups have been investigated, including folic acid,^[5] riboflavin^[6] and sugars.^{[4a,c],[7]} In this regard, biotin (see Figure 1) is a vitamin whose uptake into cancer cells is related to sodium-dependent multi-

vitamin transporter (SMVT), encoded by the *SLC5A6* gene which is overexpressed in certain cancer cell lines (e.g. breast, lung, ovarian, and renal cancer cells).^[8] Thus, biotin conjugates may be favourably captured by the tumour tissue, and this concept has been extensively used for the targeting of drugs (including drug nanocarriers^[9]) to tumours.^[10] Several classes of biotin containing metal compounds have been investigated for their anticancer potential, including complexes based on Re(I) and Ru(II),^[11] Zn(II)-phthalocyanine,^[12] Au(III)-NHC,^[13] Pt(II)^[14] and Pt(IV),^{[8b],[15]} and ferrocene derivatives.^[16] In general, such biotinylated species successfully display enhanced cellular uptake and selectivity, and the cytotoxicity and the cellular uptake are reduced when the in vitro cell medium culture is enriched with biotin or the cells are pre-treated with biotin.^[11b,8b,14a,15c]

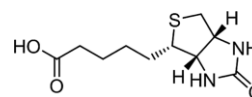


Figure 1. The structure of biotin.

Tethering biotin to metal compounds has been typically achieved by converting the biotin carboxylic acid group into amide^[11,13,14,16a] or ester^[12] linkers to subsequently generate suitable ligands. Additionally, acylation of coordinated ligands in Pt(IV)^[15] and ferrocene compounds^[8b] has been performed, as well as the direct coordination of the biotin sulfur donor atom to Ru(II) complexes.^[11c] The first Ru(II) arene-biotin conjugates were recently reported, with the biotin moiety incorporated within either the arene^[17] or a monodentate pyridine or indazole nitrogen-ligand.^[18] The nitrogen-based adducts, i.e. [RuCl₂(η⁶-*p*-cymene)(*N*-biotin)], are highly hygroscopic and slowly decompose in air, in agreement with the general tend-

[a] Dipartimento di Chimica e Chimica Industriale, Università di Pisa, Via G. Moruzzi 13, 56124 Pisa, Italy
E-mail: fabio.marchetti1974@unipi.it
<http://www.dcci.unipi.it/fabio-marchetti.html>

[b] Cytometry Lab, Department of Molecular Biophysics, Faculty of Biology and Environmental Protection, University of Łódź, ul. Pomorska 141/143, 90-236 Łódź, Poland

[c] Institut des Sciences et Ingénierie Chimiques, Ecole Polytechnique Fédérale de Lausanne (EPFL), 1015 Lausanne, Switzerland

Supporting information and ORCID(s) from the author(s) for this article are available on the WWW under <https://doi.org/10.1002/ejic.201900922>.

ency of monodentate nitrogen donor ligands to undergo easy dissociation from the Ru(II) arene centre.^[19] Instead, triarylphosphines with hydroxyl/carboxyl substituents are expected to provide a more robust anchoring to the Ru(II) centre,^[20] and are potentially derivatizable through esterification procedures.^[19a,21]

With this idea in mind, herein we present the synthesis and full characterization of biotin-conjugated Ru(II) arene compounds based on functionalization of an aryl-diphenylphosphine ligand. The stability of the compounds in aqueous media (including cell culture medium), their avidin affinity and anti-proliferative activity against a panel of tumorigenic cell lines, with differentiated *SLC5A6* expression levels, were investigated.

Results and Discussion

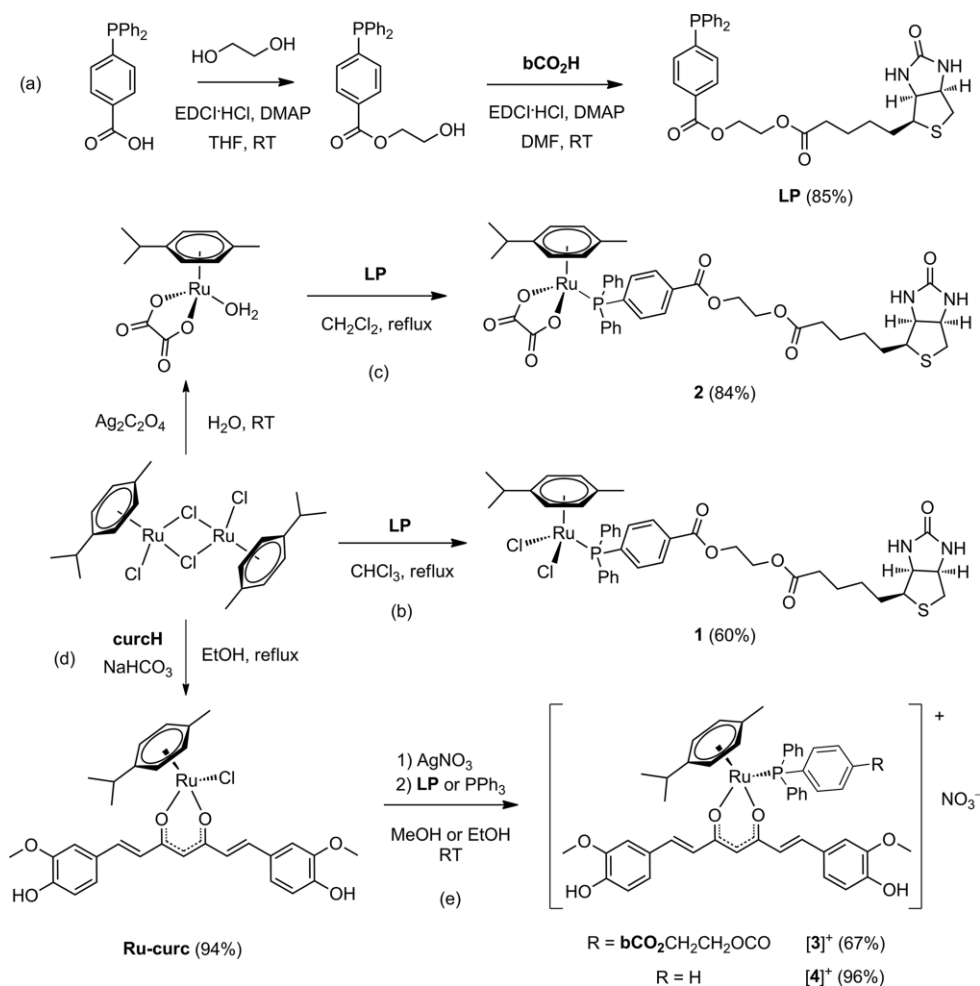
1. Synthesis and Characterization of Compounds

The biotin-functionalized phosphine, **LP**, was obtained via two Steglich esterification steps,^[22] starting from 4-diphenylphosphino benzoic acid, ethylene glycol and biotin (Scheme 1a). First, 4-diphenylphosphino benzoic acid was treated with an excess of ethylene glycol and EDCI/DMAP in THF, and the

mono-ester 4-Ph₂PC₆H₄CO₂(CH₂)₂OH was isolated in near-quantitative yield after chromatography. Second, esterification with biotin in DMF, followed by CH₂Cl₂/water extraction, gave **LP** as a colourless solid in 85 % yield. **LP** reacts with [RuCl₂(η⁶-*p*-cymene)]₂ in CHCl₃ under reflux or with [Ru(C₂O₄)(η⁶-*p*-cymene)(H₂O)] in CH₂Cl₂ under reflux to afford the ruthenium-biotin conjugates [RuX₂(η⁶-*p*-cymene)(**LP**)], X₂ = Cl₂ (**1**), C₂O₄ (**2**) (Scheme 1b–c). Compounds **1** and **2** were purified using chromatography and isolated as orange and yellow solids in 60 and 82 % yield, respectively.

We also investigated the incorporation of **LP** within a Ru(II) complex containing curcumin (**curcH**), i.e. another bioactive fragment of broad interest in medicinal chemistry.^[23] Curcumin behaves as a 1,3-diketonato ligand to Ru(η⁶-arene) scaffolds,^[24,25] and the known compound, [RuCl(curc)(η⁶-*p*-cymene)] (**Ru-curc**), was isolated in almost quantitative yield by a modification of the literature procedure (use of NaHCO₃ as a mild Brønsted base in refluxing ethanol, see Scheme 1d).^[24,25a]

Treatment of **Ru-curc** with AgNO₃ and then **LP** in MeOH affords the ruthenium-biotin-curcumin conjugate [Ru(curc)(η⁶-*p*-cymene)(**LP**)]NO₃, [**3**]⁺NO₃ (Scheme 1e), which was isolated as a red solid in 67 % yield following chromatography (NaNO₃-saturated MeOH used as eluent). The analogous triphenylphos-



Scheme 1. Synthetic routes to biotin-functionalized phosphine ligand **LP** (a), Ru complexes [RuX₂(η⁶-*p*-cymene)(**LP**)] (X₂ = Cl₂, **1**; C₂O₄, **2**) (b, c), [RuCl(curc)(η⁶-*p*-cymene)] (**Ru-curc**) (d) and related phosphine derivatives [Ru(curc)(η⁶-*p*-cymene)(PR₃)]NO₃ (PR₃ = **LP**, [**3**]⁺; PPh₃, [**4**]⁺) (e). **bCO**₂H = biotin; **curcH** = curcumin.

phine derivative, **[4]NO₃**, was prepared using a similar procedure (96 % yield, Scheme 1e).

The novel Ru compounds **1**–**[4]NO₃** are air and moisture stable solids, whereas **LP** slowly converts to the phosphine oxide (**O=LP**) upon air exposure in the solid state or in solution. Compounds **1**–**[4]NO₃** are soluble in common polar organic solvents (CH₂Cl₂, MeOH, DMSO, acetone), but show no appreciable solubility in water, despite the presence of hydrogen bonded donor groups [CO(NH)₂, ArOH] and the association with a hydrophilic anion (NO₃[−]).

All the new compounds were characterized by analytical (CHN analysis, conductivity and mass spectrometry) and spectroscopic (IR, NMR and UV/Vis) techniques, with selected data compiled in Tables S1–S2 and NMR and IR spectra given in Figures S1–S24 (SI). NMR spectra of **LP** and Ru compounds **1**–**[4]NO₃** in CD₃OD, CDCl₃ or [D₆]acetone show resonances that are fully consistent with the proposed structures.^[26] Complexes **1**–**[4]**⁺ exhibit a downfield shifted ³¹P NMR signal (25–34 ppm vs. –5 ppm in **LP**/PPh₃) and an increased ¹J_{CP} coupling constant (42–47 Hz vs. 10–15 Hz in **LP**/PPh₃), that are diagnostic features for coordination of arylphosphine ligands to the {(η⁶-arene)Ru} frame.^[27] The oxalato ligand in **2** has strong C=O stretching bands in the 1650–1690 cm^{−1} region of the IR spectrum and a ¹³C NMR signal at 167 ppm.^[20a,28] Strong IR absorptions related to the ureide and ester C=O groups are in the range 1690–1725 cm^{−1} for **LP** and **1**–**[3]**⁺. The spectroscopic features of the biotinyl fragment are very similar in biotin itself and derivatives **LP** and **1**–**[3]**⁺. This similarity indicates that there are not significant interactions between the Ru ions and biotin fragment, in particular with the sulfur atom (tetrahydrothiophene ring). Indeed, examples of metal complexes containing κS-coordinated biotin are rare^[29] and thioethers are often labile ligands in (η⁶-arene)Ru systems, being readily displaced by phosphines and other ligands.^[30]

¹H and ¹³C NMR resonances for the Ru-bound carbon atoms belonging to the *p*-cymene ring in **[3]**⁺ and **[4]**⁺ are considerably deshielded with respect to the neutral precursor **Ru-curc**. Conversely, ¹H NMR signals for the alkenyl and HC(CO)₂ protons of the curcuminato ligand in **Ru-curc** move to lower ppm values in the cationic derivatives.^[31] The [NO₃][−] ion within **[3]NO₃** and **[4]NO₃** gives rise to a signal at −3.5 ppm in the ¹⁴N NMR spectra^[32,33] (in CD₃OD), and a strong band around 1320–1330 cm^{−1} in the IR spectra.^[34] In the UV/Vis spectra, curcumin-functionalized complexes **[3]**⁺ and **[4]**⁺ display intense (ε ≈ 3 × 10⁴ cm^{−1} M^{−1}) bands at ca. 410, 450, 480 nm, shifted to longer wavelengths with respect to their neutral chlorido precursor **Ru-curc** and curcumin.^[24a]

2. Stability of the Complexes in DMSO/Water and Cell Culture Medium

An assessment of the stability of metal compounds in simple aqueous medium is essential to evaluate their suitability for biological studies.^[35] Biological tests for water insoluble compounds often rely on the use of DMSO,^[36] however DMSO is a good ligand for ruthenium(II)^[37] and can cause progressive displacement of η⁶-coordinated arene,^[21a,28c,38] monodentate

(phosphine,^[28c,38d,39] pyridine/(benz)imidazole/indazole^[40]) and bidentate (carboxylate,^[41] diketone^[38b,38e,42]) ligands. In general, (η⁶-arene)Ru-phosphine complexes display better stability in DMSO with respect to related systems containing N-donor heterocyclic ligands (see Introduction).

The stability of **1**–**[4]**⁺ was evaluated in a DMSO:water 7:3 v/v mixture, and the same study was extended to the previously reported compound **Ru-curc** as a reference. Solutions of the compounds were maintained at 37 °C for 72 hours and periodically analyzed by NMR spectroscopy and conductivity measurements (see Tables S3–S7 and Schemes S3–S7 in the SI). The (%) fraction of starting material detected in solution over time is shown in Table 1. Only minor amounts of *p*-cymene and **O=LP** were slowly released from **2** and **[3]**⁺, with these compounds being more robust than **1** and **Ru-curc** (82–89 % of the starting material was recognized in solution after 72 hours, see Table 1 and SI for details). Release of O=PPh₃ from **[4]**⁺ occurred to a higher extent than **O=LP** from **2** and **[3]**⁺, but is significantly inhibited with respect to the situation in [RuCl₂(η⁶-*p*-cymene)(PPh₃)] (30 % after 72 hours).^[20a] These results well agree with the improved solvolytic stability manifested by [Ru(O,O')(η⁶-arene)(PR₃)^{0/+}] complexes with respect to related [RuCl₂(η⁶-arene)(PR₃)] and [RuCl(O,O')(η⁶-arene)] systems (O,O' = 1,2-dicarboxylate,^[28b-c,43] 1,3-diketone^[44b]). On account of these preliminary results, **1** was excluded from further stability and biological studies.

Table 1. Fraction of starting material in DMSO:D₂O 7:3 v/v solutions of Ru complexes over time; % values are based on ¹H NMR (Me₂SO₂ internal standard).

Compound	0 h ^[a]	24 h	48 h	72 h
1	85	62	–	56
2	100	97	94	89
[3]NO₃	100	99	89	82
[4]NO₃	100	80		64
Ru-curc		≤ 76	≤ 70	≤ 57

[a] NMR spectra were recorded shortly after dissolution (*t* < 10 min).

Little attention has been given up to now to the stability and speciation of Ru-arene complexes in cell culture media.^[35,45] We investigated the stability of **2** and **[3]NO₃** in DMSO/RPMI 1640 cell culture medium mixtures. Accordingly, solutions of **2** and **[3]NO₃** (1.8 mM) were maintained at 37 °C for 72 hours and monitored via ³¹P{¹H} NMR spectroscopy (see SI for details). The freshly prepared solutions feature a single ³¹P NMR signal corresponding to the starting material (**2**: 35.8 ppm; **[3]**⁺: 36.0 ppm). The relative intensity of this signal progressively decreased over time and new peaks appeared in the region 36–32 ppm. After 72 h, the solution was diluted with water and extracted with CH₂Cl₂. Complexes **2** and **[3]**⁺ were identified by NMR in the residue of the organic phase, together with **O=LP** and curcumin (in the latter case). In summary, the stability experiments showed that two Ru-arene complexes, which are substantially stable in DMSO/water mixtures and do not possess ligands prone to hydrolysis (e.g. Cl[−]), nevertheless undergo some modifications when incubated at 37 °C in the cell culture medium, with a slow, partial release of the bioactive components. This behaviour may be functional to the activation of the complexes,

as previously demonstrated for leading Ru(II)-arene compounds by means of extensive investigations.^[46–51]

3. Interaction of the Compounds with Avidin

Avidin is a tetrameric egg white protein with an extremely high affinity for D-biotin and therefore used as a model biotin receptor.^[18,52] The apparent affinity of the investigated compounds to avidin was measured using a substitution assay (FluoReporter® Biotin Quantitation Assay Kit) to determine the apparent dissociation constant (K_d), maximum binding capacity (B_{max}) and Hill coefficient (H) (Table 2). Compound **2** exhibits the highest affinity towards avidin in such an experimental setup (K_d of 925 nM vs. 350 nM for biotin), followed by **LP** and **[3]NO₃**. As expected, **[4]NO₃** (which does not contain the biotin frame) does not interact with avidin.

Table 2. Apparent kinetic characteristics of investigated Ru-biotin complexes binding to avidin. The results are presented as means \pm half-width of their respective 95 % confidence intervals. Calculations were performed on data obtained in three independent experiments. N/A – not applicable.

	K_d [μ M]	B_{max} [AU]	H [1/7]
LP	4.3 ± 1.3	14.8 ± 1.7	1.3 ± 0.4
2	0.93 ± 0.09	6.9 ± 0.3	3.0 ± 0.8
[3]NO₃	9.7 ± 2.6	3.5 ± 0.7	2.6 ± 1.7
[4]NO₃	N/A	N/A	N/A
biotin	0.35 ± 0.05	17.6 ± 1.1	4.5 ± 1.3

4. Cytotoxicity Studies

The ligand **LP** and the complexes **2** and **[3]NO₃** were initially assessed for their cytotoxicity against cisplatin sensitive (A2780) and cisplatin resistant human ovarian carcinoma (A2780cisR) cell lines (Table 3), as these two cell lines are widely used to study new putative metal drugs and are therefore ideal for benchmarking. Cisplatin and **[RuCl₂(η^6 -*p*-cymene)(κ P-pta)]** (RAPTA-C)^[53] were evaluated as positive and negative controls, respectively. Compound **2** exhibited a modest cytotoxicity, while **[3]NO₃** is inactive against the tested cell lines. The observed lack of cytotoxicity is reminiscent of RAPTA-C and other RAPTA-type complexes.^[54] It should be noted that Ru(II) compounds with similar triphenylphosphine ligands functionalized with a bioactive group displayed IC_{50} values ranging from low micromolar to almost inactive in the same cancer cell

Table 3. IC_{50} values (μ M) obtained for **LP**, **2**, **[3]NO₃** and reference metal compounds on cancer (A2780, A2780cisR) cells at 72 hours (RPMI 1640 medium). Values are given as the mean \pm SD.

Compound	A2780	A2780cisR
curcH ^[24b]	ca. 6	ca. 20
Ru-curc ^[24b]	23 ± 3	27 ± 3
LP	41 ± 8	58 ± 11
2	107 ± 14	105 ± 9
[3]NO₃	> 200	> 200
RAPTA-C	> 200	> 200
cisplatin	2.3 ± 0.6	31 ± 3

lines.^[21a,55] Interestingly, sub-micromolar IC_{50} values were obtained on A2780/A2780cisR cell lines upon introduction of a pta ligand (in the place of **LP**, as in **[3]NO₃**) to the **[RuCl(η^6 -*p*-cymene)(curc)]** scaffold.^[25a]

Next, we decided to extend the biological studies to three other cancer cell lines, namely COLO 205 and SW620 (human colorectal adenocarcinoma) and HCT 116 (human colorectal carcinoma). In order to probe the role of the biotin fragment in **LP**, **2** and **[3]NO₃**, the relative SLC5A6 (AKA SMVT) protein content in the plasma membranes in the COLO 205, SW620 and HCT 116 cell lines was determined using the anti-SLC5A6 antibody (Figure 2).

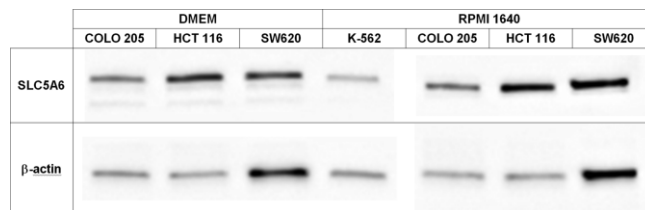


Figure 2. Western blot analysis of SLC5A6 expression in selected cancer cell lines cultured in high- and low-biotin media (DMEM and RPMI1640, respectively). K562 cell lysate was used as a positive control. β -actin (a product of an established housekeeping gene) was used as a loading control to enable inter-lane comparisons.

Densitometry analysis (Table 4) revealed that the protein abundance pattern is different from the mRNA expression pattern reported previously.^[18] The highest SLC5A6 level was found in HCT 116 cells, followed by COLO 205 and SW620, and the trend does not seem to be significantly affected by the cell culture medium. This suggests that even low biotin levels, derived from foetal bovine serum used for medium supplementation (FBS biotin content is 35 ± 4 μ g/mL which equals to 0.014 ± 0.002 μ M in the final medium composition)^[56] are high enough to maintain the expression pattern of the major biotin transporter.

Table 4. Densitometry analysis of SLC5A6 expression in selected cancer cell lines. SLC5A6 signal volume was normalized to corresponding β -actin signal volume. K562 cell lysate was used as a positive control.

Medium	Cell line	Normalized SLC5A6 signal
RPMI 1640	COLO 205	1.698
	HCT 116	3.774
	SW620	1.087
DMEM	K562	0.492
	COLO 205	1.062
	HCT 116	2.880
	SW620	0.534

The antiproliferative potential of **LP**, **2**, **[3]NO₃** and **[4]NO₃** was comparatively assessed against COLO 205, HCT 116, and SW620 cancer cell lines both in biotin-rich RPMI 1640 medium (biotin concentration = 0.8 μ M) and in essentially biotin-free DMEM (Table 5).^[57]

Notably, the cytotoxicity of the investigated compounds was significantly enhanced in DMEM (which does not contain biotin), with IC_{50} values being up to two orders of magnitude lower than the corresponding values determined in RPMI 1640. Inter-

Table 5. IC₅₀ values (μM) obtained for **LP**, **2**, **[3]NO₃** and **[4]NO₃** on cancer cells at 72 hours, in DMEM (top) and RPMI 1640 (bottom) media. Values are given as the means along with their respective 95 % confidence intervals (lower line).

	HCT 116	COLO 205	SW620
LP	1.014 0.825–1.245	0.921 0.790–1.073	0.838 0.677–1.036
2	2.809 2.210–3.570	2.839 2.438–3.307	3.253 2.709–3.906
[3]NO₃	1.967 1.319–2.933	0.828 0.685–1.000	2.783 1.829–4.235
[4]NO₃	1.817 1.387–2.379	2.326 1.546–3.499	2.330 1.744–3.115
LP	5.850 4.131–8.285	2.983 2.540–3.503	3.319 2.936–3.752
2	84.86 39.13–184.00	> 200 > 200	72.68 44.94–117.50
[3]NO₃	16.33 11.31–23.56	6.672 4.954–8.986	10.29 8.407–12.58
[4]NO₃	22.68 17.33–29.69	142.80 48.09–423.90	101.30 39.54–259.40

estingly, such a relation was observed also for **[4]NO₃**, which is not a biotin derivative. The overall sensitivity of colon cell lines towards the tested compounds approximates to COLO 205 (most sensitive) > SW620 ≥ HCT116 (least sensitive) in DMEM and SW620 > HCT 116 ≥ COLO 205 in RPMI 1640, respectively. Although a correlation between SLC5A6 expression and compound sensitivity was not apparent, the trend in antiproliferative activity is the same in both cell culture media, and in all cases the activity is higher in the biotin-free DMEM cell culture conditions.

Conclusions

Biotin is an essential micronutrient^[58] preferentially taken up by certain cancers, and therefore by using biotin as a targeting vector to introduce cytotoxins into cancer cells represents a promising chemotherapy approach. We prepared and characterized a series of Ru(II) arene compounds containing a biotin fragment tethered to the metal centre via a biotin-functionalized triphenylphosphine ligand. One of the compound also included curcumin as a second, biologically active fragment. Notably, two of the complexes exhibited excellent stability in dmsO/water mixtures, and slow degradation in cell culture medium, potentially providing a mechanism for drug activation. The observed cytotoxicity of the biotin-containing metal complexes is not correlated with SLC5A6 protein expression, which has been noted also in other studies^[8b,13,18] However, the investigated compounds are able to interact with a model biotin receptor (avidin), and their antiproliferative activity is higher when biotin is absent from the cell culture medium.

Experimental Section

1. General Experimental Details

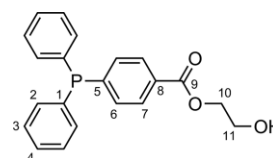
Chemicals: RuCl₃·xH₂O was purchased from Chimet S.p.A., while other reactants and solvents were obtained from Alfa Aesar, Sigma

Aldrich or TCI Europe and were of the highest purity available. Biotin (**bCO₂H**), 4-(diphenylphosphino)benzoic acid, and ethylene glycol were stored under N₂; curcumin (**curCH**) and ethyl(diisopropylamino)carboxydiimide hydrochloride (EDCI·HCl) were stored under N₂ at – 20 °C. Silica gel (Merck, 70–230 mesh) was used for column chromatography. Compounds [RuCl₂(η⁶-*p*-cymene)(pta)] (RAPTA-C),^[59] [RuCl₂(η⁶-*p*-cymene)]₂^[60] and [Ru(C₂O₄)(η⁶-*p*-cymene)(H₂O)]^[28b,28c] were prepared according to the literature. The syntheses of 4-Ph₂PC₆H₄CO₂(CH₂)₂OH, **LP** and **1-[3]NO₃** were performed under N₂ using standard Schlenk techniques and solvents distilled from appropriate drying agents (DMF from BaO, THF from CaH₂, CH₂Cl₂, CHCl₃ from P₂O₅). Once isolated, 4-Ph₂PC₆H₄CO₂(CH₂)₂OH and **LP** were stored under N₂, all the other compounds being air- and moisture-stable in the solid state. All the other operations were carried out in air with common laboratory glassware. NMR spectra were recorded at 25 °C on a Bruker Avance II DRX400 instrument equipped with a BBFO broadband probe. Chemical shifts (expressed in parts per million) are referenced to the residual solvent peaks^[61] (¹H, ¹³C) or to external standards^[62] (¹⁴N to CH₃NO₂, ³¹P to 85 % H₃PO₄, ³⁵Cl to 1 M NaCl in D₂O). In [D₆]DMSO:D₂O mixtures, chemical shifts were referenced to the residual peak as in pure [D₆]DMSO. ¹H and ¹³C spectra were assigned with the assistance of ¹H{³¹P}, ¹³C DEPT 135, ¹H-¹H COSY, ¹H-¹³C *gs*-HSQC and ¹H-¹³C *gs*-HMBC experiments.^[63] CDCl₃ stored in the dark over Na₂CO₃ was used for NMR analysis. IR spectra (650–4000 cm⁻¹) were recorded on a Perkin Elmer Spectrum One FT-IR spectrometer, equipped with a UATR sampling accessory. UV/Vis spectra (190–900 nm) were recorded on a Ultraspec 2100 Pro spectrophotometer with 0.1 cm quartz cuvettes. IR and UV/Vis spectra were processed with Spectragryph software.^[64] Carbon, hydrogen and nitrogen analyses were performed on a Vario MICRO cube instrument (Elementar). Conductivity measurements^[65,66] were carried out at 23 °C using an XS COND 8 instrument (cell constant = 1.0 cm⁻¹).

Biologicals: Inorganic salts, acids and bases used for biological assays were purchased from Avantor Performance Materials Poland (Gliwice, Poland) or Chempur (Piekary Śląskie, Poland). Anti-β-actin antibody (clone AC-74), MTT, SDS, and DMSO were obtained from Sigma-Aldrich (Saint Louis, MO USA). FluoReporter® Biotin Quantitation Assay Kit, enhanced chemiluminescence detection system Super Signal West Dura Extended Duration Substrate, foetal bovine serum, trypsin/EDTA solution and culture media were purchased from Thermo Fisher Scientific Inc. (Waltham, MA USA). Ready Gel precast gels were obtained from Bio-Rad (Richmond, CA USA). Anti-SLC5A6 (murine IgM kappa light chain, clone D-11) and corresponding HRP-conjugated secondary antibody (murine IgGκ BP-HRP) were provided by Santa Cruz Biotechnology (Dallas, TX USA). All buffers and aqueous solutions were prepared using Milli-Q water (Milli-Q Integral water station, Millipore, Billerica, MA USA).

2. Synthesis and Characterization of Compounds

2-Hydroxyethyl-4-(diphenylphosphanyl)benzoate, 4-Ph₂PC₆H₄-CO₂(CH₂)₂OH (Scheme 2)

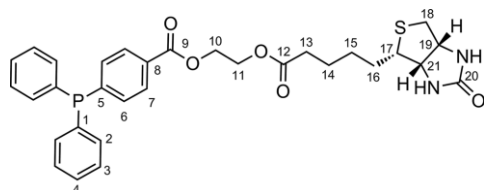


Scheme 2. Structure of 4-Ph₂PC₆H₄CO₂(CH₂)₂OH (numbering refers to C atoms).

In a 25-mL Schlenk tube under N₂, 4-(diphenylphosphino)benzoic acid (243 mg, 0.793 mmol), DMAP (19 mg, 0.16 mmol), EDCl·HCl (170 mg, 0.887 mmol), THF (10 mL) and ethylene glycol (0.50 mL, 9.0 mmol) were introduced. The colourless opalescent solution was stirred at room temperature for 3 hours, then volatiles were removed under vacuum. The residue was suspended in CH₂Cl₂ (15 mL) and extracted with H₂O (3 × 20 mL). The organic phase was concentrated under vacuum then moved on top of a silica column (h 4, d 3 cm). Impurities were eluted with CH₂Cl₂ (30 mL) then the title compound was eluted with CH₂Cl₂/Et₂O = 6:1 v/v (200 mL). Volatiles were removed under vacuum; the resulting colourless oily residue was dried under vacuum over P₂O₅ and stored under N₂. Yield: 260 mg, 93 %. Compound 4-Ph₂PC₆H₄CO₂(CH₂)₂OH is soluble in CH₂Cl₂, CHCl₃, acetone, poorly soluble in Et₂O. IR (solid state): $\bar{\nu}$ /cm⁻¹ = 3430w-br (ν_{OH}), 3069w, 3053w, 3029w, 3016w, 3002w, 2953w, 2927w, 2872w; 1716s, 1700m-sh (ν_{C=O}), 1596m, 1585m-sh, 1558w, 1479m, 1454w, 1434m, 1394m, 1372m-sh, 1329m, 1309m, 1267s-br, 1182m, 1157w, 1122s, 1112m-sh, 1085s, 1070s, 1017s, 999m, 903m, 851m, 762m, 742s, 719m, 693s. ¹H NMR (CDCl₃): δ /ppm = 7.99 (d, ³J_{HH} = 7.4 Hz, 2H, C7-H), 7.40–7.32 (m, 12H, C6-H + Ph), 4.48–4.42 (m, 2H, C10-H), 3.94–3.90 (m, 2H, C11-H), 2.55 (s-br, 1H, OH). ¹³C{¹H} NMR (CDCl₃): δ /ppm = 166.6 (C9), 144.2 (d, ¹J_{CP} = 14 Hz, C5), 135.9 (d, ¹J_{CP} = 10 Hz, C1), 133.9 (d, ²J_{CP} = 20 Hz, C2), 133.1 (d, ²J_{CP} = 19 Hz, C6), 129.7 (C8), 129.3 (d, ³J_{CP} = 6 Hz, C7), 128.6 (d, ³J_{CP} = 7 Hz, C3), 129.1 (C4), 66.5 (C10), 60.8 (C11). ³¹P{¹H} NMR (CDCl₃): δ /ppm = -5.1.

2-Hydroxyethyl 4-(diphenylphosphoryl)benzoate, 4-Ph₂P(=O)C₆H₄CO₂(CH₂)₂OH. Formation of the phosphine oxide upon air exposure during workup is negligible except during column chromatography, which has to be performed under N₂ with deaerated solvents. ¹H NMR (CDCl₃): δ /ppm = 8.14 (d, ³J_{HH} = 6.6 Hz, C7-H). ³¹P{¹H} NMR (CDCl₃): δ /ppm = 29.3.

2-(Biotinyloxy)ethyl 4-(diphenylphosphanyl)benzoate, LP (Scheme 3)



Scheme 3. Structure of LP (numbering refers to C atoms).

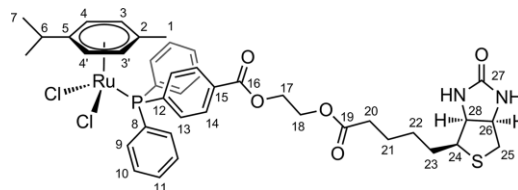
In a 25-mL Schlenk tube under N₂, 4-Ph₂PC₆H₄CO₂(CH₂)₂OH (260 mg, 0.742 mmol), bCO₂H (229 mg, 0.937 mmol), DMAP (19 mg, 0.16 mmol), EDCl·HCl (180 mg, 0.939 mmol) and DMF (6 mL) were introduced and the colourless solution was stirred at room temperature. After 6 hours, the conversion was checked by ¹H NMR (CDCl₃) and volatiles were removed under vacuum. The oily residue was dissolved in CH₂Cl₂ (10 mL) and extracted with H₂O (3 × 20 mL). The organic phase was taken to dryness under vacuum affording the title compound as a colourless foamy solid. The solid was washed with petroleum ether, dried under vacuum over P₂O₅ and stored under N₂. Yield: 364 mg, 85 %. Compound LP is soluble in CH₂Cl₂, CHCl₃, MeOH, acetone, less soluble in Et₂O; insoluble in hydrocarbons and water. Anal. Calcd. for C₃₁H₃₃N₂O₅PS: C, 64.57; H, 5.77; N, 4.85; found C, 64.39; H, 5.68; N, 4.94. ESI-MS(+): m/z found 577.1934 [M + H⁺], calcd. for C₃₁H₃₄N₂O₅PS 577.1926; the isotopic pattern fits well the calculated one. IR (solid state): $\bar{\nu}$ /cm⁻¹ = 3380w-sh, 3216w (ν_{NH}); 3069w, 3054w, 3055w, 2961w, 2922w, 2862w, 1717s (ν_{C=O}), 1694s (ν_{C12=O} + ν_{C20=O}), 1596m, 1585w-sh, 1558w,

1479w, 1453m, 1434m, 1394m, 1374w, 1332w, 1309w, 1262s, 1240m-sh, 1179m, 1120m-sh, 1105s, 1085s, 1017m, 999m-sh, 922w, 852m, 802m, 761m, 744s, 720m, 695s. UV/Vis (MeOH, 1.6 × 10⁻³ M): λ_{max} (ε /cm⁻¹ × M⁻¹) = 289 (1.1 × 10⁴). ¹H NMR (CD₃OD): δ /ppm = 7.94 (d, ³J_{HH} = 7.4 Hz, 2H, C7-H), 7.39–7.27 (m, 12H, C6-H + Ph), 4.53–4.49 (m, 2H, C10-H), 4.44–4.38 (m, 3H, C11-H + C19-H), 4.17 (dd, ³J_{HH} = 7.8, 4.5 Hz, 1H, C21-H), 3.07–3.02 (m, 1H, C17-H), 2.82 (dd, ²J_{HH} = 12.8 Hz, ³J_{HH} = 4.9 Hz, 1H, C18-H), 2.64 (d, ²J_{HH} = 12.7 Hz, 1H, C18-H'), 2.35 (t, ³J_{HH} = 7.2 Hz, 2H, C13-H), 1.71–1.59 (m, 3H, C14-H + C16-H), 1.58–1.47 (m, 1H, C16-H'), 1.43–1.35 (m, 2H, C15-H). ¹³C{¹H} NMR (CD₃OD): δ /ppm = 175.1 (C12), 167.4 (C9), 166.0 (C20), 146.1 (d, ¹J_{CP} = 15 Hz, C5), 137.5 (d, ¹J_{CP} = 11 Hz, C1), 135.0 (d, ²J_{CP} = 20 Hz, C2), 134.2 (d, ²J_{CP} = 19 Hz, C6), 129.9 (d, ³J_{CP} = 7 Hz, C3), 131.1 (C8), 130.4–130.3 (m, C4 + C7), 64.2 (C10), 63.28 (C21), 63.26 (C11), 61.6 (C19), 56.9 (C17), 41.1 (C18), 34.7 (C13), 29.6 + 29.4 (C15 + C16), 25.9 (C14). ³¹P{¹H} NMR (CD₃OD): δ /ppm = -5.2 ppm. ¹H NMR (CDCl₃): δ /ppm = 7.96 (dd, ³J_{HH} = 8.3 Hz, ⁴J_{HP} = 1.3 Hz, 2H, C7-H), 7.39–7.26 (m, 12H, C6-H + Ph), 6.18 (s, 1H, NH), 5.76 (s, 1H, N'H), 4.52–4.47 (m, 2H, C10-H), 4.43–4.36 (m, 3H, C11-H + C19-H), 4.22 (dd, ³J_{HH} = 6.8, 4.9 Hz, 1H, C21), 3.09–3.04 (m, 1H, C17), 2.81 (dd, ²J_{HH} = 12.8 Hz, ³J_{HH} = 4.9 Hz, 1H, C18-H), 2.68 (d, ²J_{HH} = 12.7 Hz, 1H, C18-H), 2.34 (t, ³J_{HH} = 7.5 Hz, 2H, C13-H), 1.72–1.57 (m, 4H, C14-H + C16-H), 1.45–1.36 (m, 2H, C15-H). ³¹P{¹H} NMR (CDCl₃): δ /ppm = -5.0.

2-(Biotinyloxy)ethyl 4-(diphenylphosphoryl)benzoate, O=LP.

Formation of the phosphine oxide upon air exposure during workup is negligible, except during (possible) column chromatography, which has to be performed under N₂ with deaerated solvents. Chromatography is not necessary if the precursor 4-Ph₂PC₆H₄CO₂(CH₂)₂OH is free from phosphine/phosphine oxide impurities. ¹H NMR (CD₃OD): δ /ppm = 8.19 (dd, ³J_{HH} = 8.0 Hz, ⁴J_{HP} = 2.0 Hz, 2H, C7-H), 7.81 (dd, ³J_{HP} = 11.6 Hz, ³J_{HH} = 8.3 Hz, 2H, C6-H), 7.73–7.65 (m, 6H, C3-H + C4-H), 7.64–7.56 (m, 4H, C2-H). All the other signals are superimposable to those of LP. ³¹P{¹H} NMR (CD₃OD): δ /ppm = 31.4. ¹H NMR (CDCl₃): δ /ppm = 8.11 (dd, ³J_{HH} = 8.4 Hz, ⁴J_{HP} = 2.5 Hz, 2H, C7-H). ³¹P{¹H} NMR (CDCl₃): δ /ppm = 28.6.

[RuCl₂(η⁶-p-cymene)(LP)], 1 (Scheme 4)

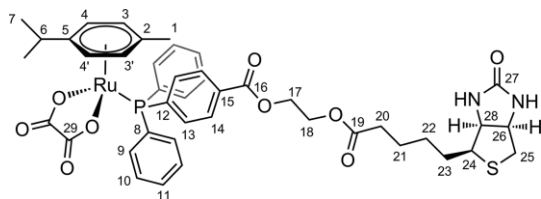


Scheme 4. Structure of 1 (numbering refers to C atoms).

In a 25-mL Schlenk tube under N₂, a dark red solution of [RuCl₂(η⁶-p-cymene)₂ (40 mg, 0.65 mmol) and LP (79 mg, 0.137 mmol) in CHCl₃ (10 mL) was stirred at reflux temperature. After 6 hours, the conversion was checked by ¹H NMR (CDCl₃) and the dark cherry-red opalescent solution was cooled to room temperature. The solution was concentrated under vacuum then moved on top of a SiO₂ column (h 6, d 2.3 cm). Impurities were eluted with CH₂Cl₂/acetone mixtures (gradient from 1:0 to 1:2 v/v) then an orange band was collected with CH₂Cl₂/acetone/MeOH (15:30:2 v/v/v, ca. 150 mL). Volatiles were removed under vacuum and the residue was suspended in Et₂O. The suspension was filtered and the resulting orange solid was washed with Et₂O and dried under vacuum (40 °C). Yield: 69 mg, 60 %. Compound 1 is soluble in DMSO, DMF, CH₂Cl₂, CHCl₃, poorly soluble in acetone, MeCN, almost insoluble in MeOH, insoluble in Et₂O, water. Anal. Calcd. for C₄₃H₄₇N₂O₉PRuS: C, 55.78;

H, 5.37; N, 3.17; found C, 55.84; H, 5.32; N, 3.24. ESI-MS(+): m/z found 901.1281 [M + H⁺], calcd. for C₄₃H₄₈N₂O₉PRuS 901.1861; the isotopic pattern fits well the calculated one. IR (solid state): $\tilde{\nu}$ /cm⁻¹ = 3280w-br (ν_{NH}), 3057w, 2958w-sh, 2926m, 2869w-sh, 1715s-sh ($\nu_{\text{C16=O}}$), 1697s-br ($\nu_{\text{C19=O}} + \nu_{\text{C27=O}}$), 1598m, 1483m-sh, 1463m-sh, 1454m-sh, 1435m, 1395m, 1376m, 1331m, 1316m, 1268s-br, 1184m, 1161m, 1126m, 1111m, 1088s, 1058m-sh, 1018m, 1000w-sh, 952w, 926w, 886w-sh, 858m, 800w, 762m, 751m, 722m, 696s. Λ_m (acetone, 1.2 × 10⁻³ M): 5 S cm⁻² mol⁻¹. UV/Vis (CH₂Cl₂, 1.2 × 10⁻³ M): λ/nm (ϵ / M⁻¹ cm⁻¹) = 378 (1.4 × 10³), 480sh (4.7 × 10²). ¹H NMR (CDCl₃): δ /ppm = δ /ppm = 7.92–7.89, 7.84–7.77 (m, 8H, Ph/C₆H₄), 7.48–7.38 (m, 6H, Ph/C₆H₄), 5.46 (s-br, 1H, NH), 5.28 (d, ³J_{HH} = 6.3 Hz, 1H, C4-H), 5.25 (d, ³J_{HH} = 5.9 Hz, 1H, C4'-H), 5.05 (d, ³J_{HH} = 5.6 Hz, 1H, C3-H'), 4.98 (d, ³J_{HH} = 5.6 Hz, 1H, C3-H), 4.92 (s-br, 1H, N'H), 4.51–4.41 (m, 3H, C17-H + C26-H), 4.41–4.34 (m, 2H, C18-H), 4.31–4.26 (m, 1H, C28-H), 3.13–3.04 (m, 1H, C24-H), 2.91–2.79 (m, 2H, C6-H + C25-H), 2.70–2.61 (m, 1H, C25-H'), 2.33 (t, ³J_{HH} = 7.0 Hz, 2H, C20-H), 1.86 (s, 3H, C1-H), 1.70–1.60 (m, 4H, C21-H + C23-H), 1.49–1.35 (m, 2H, C22-H), 1.11 (d, ³J_{HH} = 6.9 Hz, 6H, C7-H). ¹H NMR spectra in CDCl₃ show broadening of resonances, increasing with concentration and decreasing with time (ageing of the solution), probably related to aggregation phenomena. ¹³C{¹H} NMR (CDCl₃): δ /ppm = 173.5 (C19), 166.0 (C27), 163.4 (C16), 134.7 (d, ²J_{CP} = 9 Hz, C13), 134.4 (app. t, ²J_{CP} = 9 Hz, C9), 128.7 (d, ³J_{CP} = 10 Hz, C14), 128.4 (d, ³J_{CP} = 10 Hz, C10), 130.9 (C15), 130.8 (C11), 111.6 (C5), 96.6 (C2), 89.0 (C4 + C4'), 87.6, 87.5 (d, ³J_{CP} = 4 Hz, C3 + C3'), 63.0 (C28); 62.2, 62.1, 60.1 (C17 + C18 + C26), 55.6 (C24), 40.7 (C25), 34.0 (C20), 30.5 (C6); 28.54, 28.45 (C22 + C23), 25.0 (C21); 22.04, 21.97 (C7), 17.9 (C1). ³¹P{¹H} NMR (CDCl₃): δ /ppm = 25.5. ¹H NMR ([D₆]acetone): δ /ppm = 8.08–8.02, 7.94–7.89 (m, 8H, Ph + C₆H₄), 7.52–7.43 (m, 6H, Ph + C₆H₄), 5.70 (s-br, 1H, NH), 5.59 (s-br, 1H, N'H); 5.35, 5.32 (d, ³J_{HH} = 6.1 Hz, 2H, C4-H + C4'-H); 5.25, 5.22 (d, ³J_{HH} = 6.1 Hz, 2H, C3-H + C3'-H), 4.54–4.50 (m, 2H, C17-H), 4.48–4.40 (m, 3H, C18-H + C26-H), 4.34–4.27 (m, 1H, C28-H), 3.20–3.12 (m, 1H, C24-H), 2.92–2.88 (m*, C25-H), 2.73–2.63 (m, 2H, C6-H + C25-H'), 2.34 (t, ³J_{HH} = 7.3 Hz, 2H, C20-H), 1.88 (s, 3H, C1-H), 1.82–1.71 (m, 1H, C23-H), 1.68–1.53 (m, 3H, C21-H + C23-H'), 1.48–1.41 (m, 2H, C22-H), 1.05 (d, ³J_{HH} = 6.9 Hz, 6H, C7-H). *Partially covered by the solvent signal. ³¹P{¹H} ([D₆]acetone): δ /ppm = 24.5.

[Ru(C₂O₄)(η^6 -*p*-cymene)(LP)], **2** (Scheme 5)

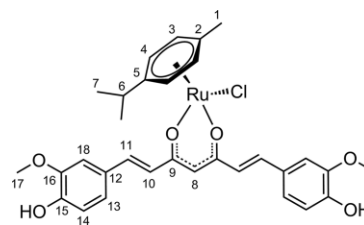


Scheme 5. Structure of **2** (numbering refers to C atoms).

In a 25-mL Schlenk tube, [Ru(C₂O₄)(η^6 -*p*-cymene)(H₂O)] (99 mg, 0.29 mmol) and **LP** (200 mg, 0.347 mmol) were dissolved in CH₂Cl₂ (5 mL). The orange solution was stirred at room temperature for 20 hours then moved on top of a silica column. Impurities were eluted with CH₂Cl₂ then a yellow band was eluted with EtOH. Volatiles were removed under vacuum and the residue was suspended in Et₂O. The suspension was filtered; the resulting yellow solid was washed with Et₂O and dried under vacuum (40 °C). Yield: 214 mg, 82 %. Compound **2** is soluble in DMSO, DMF, CH₂Cl₂, CHCl₃, MeOH, less soluble in acetone, MeCN, EtOH, insoluble in Et₂O, hexane and water. Anal. Calcd. for C₄₃H₄₇N₂O₉PRuS: C, 57.39; H, 5.26; N, 3.11; found C, 57.22; H, 5.20; N, 3.17. ESI-MS(+): m/z found 901.1866 [M

+ H⁺], calcd. for C₄₃H₄₈N₂O₉PRuS 901.1861; the isotopic pattern fits well the calculated one. IR (solid state): $\tilde{\nu}$ /cm⁻¹ = 3400w-br, 3300w-br (ν_{NH}); 3062w, 2960w, 2931w, 2869w, 1724–1715m-sh ($\nu_{\text{C16=O}}$), 1693s ($\nu_{\text{C19=O}} + \nu_{\text{C27=O}} + \nu_{\text{C29=O}}$); 1669s, 1652s ($\nu_{\text{C29=O}}$); 1600m, 1468–1460m-sh, 1435m, 1371s ($\nu_{\text{C29=O}}$), 1314m, 1268s, 1184m, 1161m, 1129m, 1113m, 1089m, 1017m, 999w, 956w, 927w, 861w, 803w, 784m, 760m, 723w, 696s. Λ_m (MeOH, 1.3 × 10⁻³ M): 6.4 S mol⁻¹ cm⁻². UV/Vis (MeOH, 1.3 × 10⁻³ M): λ/nm (ϵ / M⁻¹ cm⁻¹) = 325 (2.9 × 10³), 375 (1.2 × 10³). ¹H NMR (CD₃OD): δ /ppm = 8.03 (dd, ³J_{HH} = 8.3 Hz, ⁴J_{HP} = 1.6 Hz, 2H, C14-H), 7.65–7.53 (m, 10H, Ph), 7.51 (dd, ³J_{HP} = 10.0 Hz, ³J_{HH} = 8.6 Hz, 2H, C13-H), 5.76 (d, ³J_{HH} = 6.3 Hz, 2H, C4-H + C4'-H), 5.47–5.41 (m, 2H, C3-H + C3'-H), 4.54–4.52 (m, 2H, C17-H), 4.46–4.41 (m, 3H, C18-H + C26-H), 4.24 (dd, ³J_{HH} = 7.8, 4.5 Hz, 1H, C28-H), 3.16–3.09 (m, 1H, C24-H), 2.85 (dd, ²J_{HH} = 12.7 Hz, ³J_{HH} = 5.0 Hz, 1H, C25-H'), 2.65 (d, ²J_{HH} = 12.7 Hz, 1H, C25-H), 2.59 (hept, ³J_{HH} = 6.9 Hz, 1H, C6-H), 2.36 (t, ³J_{HH} = 7.3 Hz, 2H, C20-H), 1.93 (s, 3H, C1-H), 1.75–1.61 (m, 3H, C21-H + C23-H), 1.59–1.49 (m, 1H, C23-H'), 1.46–1.38 (m, 2H, C22-H), 1.23 (d, ³J_{HH} = 6.9 Hz, 6H, C7-H). No change in the ¹H NMR spectrum (CD₃OD) was observed after 14 h at room temperature. ¹³C{¹H} NMR (CD₃OD): δ /ppm = 175.0 (C19), 167.0 (C29), 166.8 (C16), 166.1 (C27), 136.4 (d, ¹J_{CP} = 42 Hz, C12), 135.6 (d, ²J_{CP} = 11 Hz, C9), 135.3 (d, ²J_{CP} = 10 Hz, C13), 133.3 (d, ⁴J_{CP} = 2 Hz, C15), 132.9 (d, ⁴J_{CP} = 2 Hz, C11), 130.6 (d, ³J_{CP} = 10 Hz, C14), 130.3 (d, ³J_{CP} = 10 Hz, C10), 130.3 + 130.2 (d, ¹J_{CP} = 47 Hz, C8), 109.4 (d, ²J_{CP} = 3 Hz, C5), 99.5 (C2), 89.29 + 89.28 (d, ²J_{CP} = 4 Hz, C4 + C4'), 88.1 (app. t, ²J_{CP} = 4 Hz, C3 + C3'), 64.5 (C17), 63.4 (C28), 63.2 (C18), 61.6 (C26), 56.9 (C24), 41.0 (C25), 34.7 (C20), 32.3 (C6), 29.6 + 29.4 (C22 + C23), 25.9 (C21), 22.5 (C7), 18.1 (C2), 31.3 (C6), 29.6 + 29.4 (C22 + C23), 25.9 (C21), 22.5 (C7), 18.1 (C1). ³¹P{¹H} NMR (CD₃OD): δ /ppm = 32.7 ppm. ¹H NMR (CDCl₃): δ /ppm = 7.99 (dd, ³J_{HH} = 8.0 Hz, ⁴J_{HP} = 1.2 Hz, 2H, C14-H), 7.69–7.47 (m, 10H, Ph), 7.43 (dd, ³J_{HP} = 9.8 Hz, ³J_{HH} = 8.6 Hz, 2H, C13-H); 5.53, 5.51 (d, ³J_{HH} = 6.1 Hz, 2H, C4-H + C4'-H), 5.40 (s, 1H, NH); 5.25, 5.09 (d, ³J_{HH} = 6.0 Hz, 2H, C3-H + C3'-H), 5.01 (s, 1H, N'H), 4.54–4.43 (m, 4H, C17-H + C18-H), 4.39–4.30 (m, 2H, C26-H + C28-H), 3.18–3.11 (m, 1H, C24-H), 2.87 (dd, ²J_{HH} = 12.7 Hz, ³J_{HH} = 5.1 Hz, 1H, C25-H), 2.71 (d, ²J_{HH} = 12.8 Hz, 1H, C25-H'), 2.69–2.63 (m, 1H, C6-H), 2.41–2.32 (m, 2H, C20-H), 1.90 (s, 3H, C1-H), 1.80–1.40* (m, C21-H + C22-H + C23-H), 1.22–1.18 (m, 6H, C7-H + C7'-H). *Partially covered by H₂O peak. ³¹P{¹H} NMR (CDCl₃): δ /ppm = 31.7.

[RuCl(curc)(η^6 -*p*-cymene)], **Ru-curc** (Scheme 6)

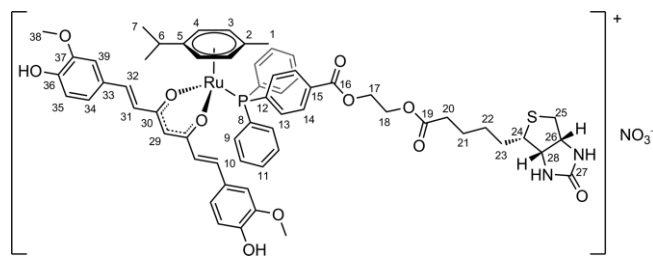


Scheme 6. Structure of **Ru-curc** (numbering refers to C atoms).

The title compound was prepared according to a modified literature procedure.^[24,25a] In a 50-mL round-bottomed flask, [RuCl₂(η^6 -*p*-cymene)]₂ (164 mg, 0.268 mmol), **curcH** (200 mg, 0.543 mmol), NaHCO₃ (46 mg, 0.55 mmol) and EtOH (15 mL) were introduced. The suspension (red-orange solution + colourless solid) was stirred in the dark at reflux temperature. After 2 hours, the conversion was checked by ¹H NMR (CDCl₃) and volatiles were removed under vacuum. The red-orange residue was suspended in acetone and filtered through a celite pad. The filtrate was taken to dryness under vacuum and the dark red residue was triturated in Et₂O. The suspension was filtered; the resulting orange-brown solid was washed with Et₂O (10 mL) and dried under vacuum (40 °C). Yield: 320 mg, 94 %.

Compound **Ru-curc** is soluble in DMSO, MeOH, EtOH, acetone, less soluble in CH₂Cl₂, CHCl₃, poorly soluble/insoluble in Et₂O, hexane. Anal. Calcd. for C₃₁H₃₃ClO₆Ru: C, 58.35; H, 5.21; found C, 58.12; H, 5.11. IR (solid state): $\tilde{\nu}$ /cm⁻¹ = 3522w, 3236w-br (ν_{OH}); 3009w, 2964w, 2929w, 2872w, 2834w; 1622w, 1603w, 1591m (ν_{OCCHCO}); 1533m-sh, 1506s (ν_{OCCHCO} + ν_{C10=C11}); 1467w, 1545w, 1429w, 1410m, 1372w, 1332w, 1286m, 1270m, 1244m, 1209m, 1177m, 1156m, 1121m, 1056w, 1033m, 1026m, 997m, 984m, 961m, 934w, 863m, 812m, 763w, 742w, 726w, 682w. UV/Vis (MeOH, 4.7 × 10⁻⁴ M): λ_{max} (ε / cm⁻¹ M⁻¹) = 264 (1.9 × 10⁴), 414 (4.3 × 10⁴), 439 (4.3 × 10⁴), 463 (4.3 × 10⁴). ¹H NMR (CDCl₃): δ /ppm = 7.53 (d, ³J_{HH} = 15.6 Hz, 2H, C11-H), 7.04 (d, ³J_{HH} = 8.5 Hz, 2H, C13-H), 7.01 (s, 2H, C18-H), 6.90 (d, ³J_{HH} = 8.2 Hz, 2H, C14-H), 6.43 (d, ³J_{HH} = 15.7 Hz, 2H, C10-H), 5.79 (s, 2H, OH), 5.56 (d, ³J_{HH} = 5.8 Hz, 2H, C4-H), 5.46 (s, 1H, C8-H), 5.29 (d, ³J_{HH} = 5.8 Hz, 2H, C3-H), 3.93 (s, 6H, C17-H), 2.98 (hept, ³J_{HH} = 6.9 Hz, 1H, C6-H), 2.35 (s, 3H, C1-H), 1.39 (d, ³J_{HH} = 6.9 Hz, 6H, C7-H). ¹H NMR ([D₆]acetone): δ /ppm = 8.04 (s, 1.2H*, OH), 7.52 (d, ³J_{HH} = 15.6 Hz, 2H, C11-H), 7.26 (s, 2H, C18-H), 7.08 (d, ³J_{HH} = 8.1 Hz, 2H, C13-H), 6.85 (d, ³J_{HH} = 8.1 Hz, 2H, C14-H), 6.55 (d, ³J_{HH} = 15.6 Hz, 2H, C10-H), 5.63 (d, ³J_{HH} = 5.7 Hz, 2H, C4-H), 5.41 (s, 1H, C8-H), 5.33 (d, ³J_{HH} = 5.6 Hz, 2H, C3-H), 3.90 (s, 6H, C17-H), 3.06–2.95 (m, 1H, C6-H), 2.27 (s, 3H, C1-H), 1.41 (d, ³J_{HH} = 6.9 Hz, 6H, C7-H). *Lower integral due to H/D exchange with residual H₂O in the solvent. ¹H NMR (CD₃OD): 7.81–7.43 (m-br, 2.5H), 7.26–6.99 (m-br, 4H), 6.82 (app. d, J = 7.5 Hz, 2.5H), 6.70–6.48 (m-br, 2H), 5.90–5.34 (m-br, 5.4H), 3.92 (s, 6H), 3.05–2.92 (m, 1H), 2.34 (s-br, 3H), 1.43 (s-br, 6H).

[Ru(curc)(η⁶-p-cymene)(LP)]NO₃, [3]NO₃ (Scheme 7)

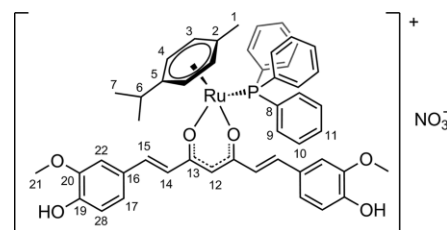


Scheme 7. Structure of [3]NO₃ (numbering refers to C atoms).

In a 25-mL Schlenk tube under N₂, [RuCl(curc)(η⁶-p-cymene)] (76 mg, 0.12 mmol), AgNO₃ (20 mg, 0.12 mmol) and MeOH (7 mL) were introduced. The mixture was stirred at room temperature in the dark for 1 hours, affording a dark red solution and a colourless solid (AgCl). Therefore **LP** (68 mg, 0.12 mmol) was added and the reaction mixture was stirred at room temperature in the dark. After 15 h, the conversion was checked by ³¹P{¹H} NMR (CDCl₃) and the suspension was filtered through a celite pad. The filtrate was concentrated under vacuum then moved on top of a silica column. Impurities were eluted with CH₂Cl₂ and EtOH, then a dark orange/red band was collected with NaNO₃-saturated MeOH as eluent. Volatiles were removed under vacuum; the residue was suspended in acetone and filtered through a celite pad. The filtrate was taken to dryness under vacuum and the residue was suspended in Et₂O. The suspension was filtered; the resulting orange solid was washed with Et₂O then dried under vacuum. Yield: 99 mg, 67 %. Compound [3]NO₃ is soluble in DMSO, DMF, MeOH, less soluble in EtOH, poorly soluble in acetone, MeCN > CH₂Cl₂, CHCl₃ and insoluble in Et₂O, hexane and water. Anal. Calcd. for C₆₂H₆₆N₃O₁₄PRuS: C, 59.99; H, 5.36; N, 3.39; found C, 59.72; H, 5.44; N, 3.26. ESI-MS(+): *m/z* found 1179.3181 [M⁺], calcd. for C₆₂H₆₆N₂O₁₁PRuS 1179.3168; the isotopic pattern fits well the calculated one. IR (solid state): $\tilde{\nu}$ /cm⁻¹ = 3400–3100w-br (ν_{NH} + ν_{OH}), 3060w, 2956w, 2935w, 2868w, 1714m

(ν_{C16=O}), 1698m (ν_{C19=O} + ν_{C27=O}); 1621m, 1598m, 1590m (ν_{OCCHCO}); 1505s, 1498s (ν_{OCCHCO} + ν_{C31=C32}), 1464m, 1435m, 1428m, 1392s, 1375s-sh, 1331m (ν_{NO3}), 1277s, 1250s-sh, 1158s, 1123s, 1094m, 1029m, 1018m, 995m, 972m, 933w, 849w, 826w, 817w, 760w, 751w, 724w, 695m. Λ_m (MeOH, 1.3 × 10⁻³ M): 86 S mol⁻¹ cm⁻². UV/Vis (MeOH, 2.6 × 10⁻⁴ M): λ/nm (ε / M⁻¹ cm⁻¹) = 250sh (3.7 × 10⁴), 410 (3.5 × 10⁴), 450 (3.3 × 10⁴), 477 (2.7 × 10⁴). ¹H NMR (CD₃OD): δ /ppm = 7.91 (dd, ³J_{HH} = 8.2 Hz, ⁴J_{HP} = 1.4 Hz, 2H, C14-H), 7.73–7.66 (m, 4H, C9-H), 7.66–7.56 (m, 6H, C10-H + C11-H), 7.48 (dd, ³J_{HP} = 10.1 Hz, ³J_{HH} = 8.6 Hz, 2H, C13-H), 7.29 (d, ³J_{HH} = 15.5 Hz, 2H, C32-H), 7.12 (s, 2H, C39-H), 7.03 (d, ³J_{HH} = 8.2 Hz, 2H, C34-H), 6.83 (d, ³J_{HH} = 7.8 Hz, 2H, C35-H), 6.36 (d, ³J_{HH} = 15.6 Hz, 2H, C31-H), 5.82 (d, ³J_{HH} = 6.2 Hz, 2H, C4-H), 5.53 (d, ³J_{HH} = 6.0 Hz, 2H, C3-H), 5.35 (s, 1H, C29-H), 4.43–4.38 (m, 3H, C17-H + C26-H), 4.37–4.33 (m, 2H, C18-H), 4.18 (dd, ³J_{HH} = 7.7, 4.5 Hz, 1H, C28-H), 3.93 (s, 6H, C38-H), 3.09–3.03 (m, 1H, C24-H), 2.79 (dd, ²J_{HH} = 12.7 Hz, ³J_{HH} = 4.9 Hz, 1H, C25-H), 2.70 (hept, ³J_{HH} = 7.0 Hz, 1H, C6-H), 2.60 (d, ²J_{HH} = 12.8 Hz, 1H, C25-H'), 2.28 (t, ³J_{HH} = 7.2 Hz, 2H, C20-H), 1.99 (s, 3H, C1-H), 1.68–1.53 (m, 3H, C21-H + C23-H), 1.52–1.43 (m, 1H, C23-H'), 1.41–1.32 (m, 2H, C22-H), 1.29 (d, ³J_{HH} = 6.9 Hz, 6H, C7-H). ¹³C{¹H} NMR (CD₃OD): δ /ppm = 181.3 (C30), 175.0 (C19), 166.7 (C16), 166.0 (C27), 150.3 (C36), 149.5 (C37), 141.5 (C32), 137.0 (d, ¹J_{CP} = 42 Hz, C12), 135.80 + 135.77 (d, ²J_{CP} = 10 Hz, C9), 135.2 (d, ²J_{CP} = 10 Hz, C13), 133.0 (d, ⁴J_{CP} = 2 Hz, C15), 132.9 (C11), 130.5 (d, ¹J_{CP} = 47 Hz, C8), 130.26 + 130.19 (d, ³J_{CP} = 10 Hz, C10 + C14), 128.8 (C33), 124.8 (C31), 124.1 (C34), 116.7 (C35), 112.1 (d, ²J_{CP} = 4 Hz, C5), 111.4 (C39), 105.9 (C29), 100.7 (C2), 90.1 (d, ²J_{CP} = 4 Hz, C4), 89.2 (d, ²J_{CP} = 2 Hz, C3), 64.5 (C17), 63.3 (C28), 63.1 (C18), 61.6 (C26), 56.9 (C24), 56.6 (C38), 41.0 (C25), 34.6 (C20), 32.1 (C6), 29.5 + 29.4 (C22 + C23), 25.9 (C21), 22.4 (C7), 17.8 (C1). ¹⁴N NMR (CD₃OD): δ /ppm = -3.6 (Δν_{1/2} = 20 Hz, NO₃⁻). ³¹P{¹H} NMR (CD₃OD): δ /ppm = 34.2.

[Ru(curc)(η⁶-p-cymene)(PPh₃)NO₃, [4]NO₃ (Scheme 8)



Scheme 8. Structure of [4]NO₃ (numbering refers to C atoms).

In a 25-mL round-bottom flask, [RuCl(curc)(η⁶-p-cymene)] (59 mg, 0.092 mmol), AgNO₃ (16 mg, 0.094 mmol) and EtOH (2 mL) were introduced. The mixture was stirred at room temperature in the dark for 1 hours, affording a dark red solution and a colourless solid (AgCl). The suspension was filtered through a celite pad then PPh₃ (27 mg, 0.10 mmol) was added to the filtrate and the solution was stirred at room temperature. After 1 h, the conversion was checked by ¹H and ³¹P{¹H} NMR (CDCl₃) then volatiles were removed under vacuum. The residue was dissolved in CH₂Cl₂ and filtered through a celite pad. The filtrate was taken to dryness under vacuum and the residue was suspended in Et₂O. The suspension was filtered; the resulting red-orange microcrystalline solid was washed with Et₂O and dried under vacuum (40 °C). Yield: 82 mg, 96 %. Compound [4]NO₃ is soluble in CH₂Cl₂, CHCl₃, MeOH, acetone, poorly soluble in EtOAc, insoluble in Et₂O. Anal. Calcd. for C₄₉H₄₈NO₉PRu: C, 63.49; H, 5.22; N, 1.51; found C, 63.59; H, 5.28; N, 1.60. ESI-MS(+): *m/z* found 865.2244 [M⁺], calcd. for C₄₉H₄₈O₆PRu 865.2232; the isotopic pattern fits well the calculated one. IR (solid state): $\tilde{\nu}$ /cm⁻¹ = 3400–2800w-br (ν_{OH}), 3053w, 3011w, 2962w, 2866w, 2839w, 1707w;

1619m-sh, 1597m, 1589m (ν_{OCCO}); 1504s, 1497s ($\nu_{\text{OCCO}} + \nu_{\text{C14-C15}}$), 1463s-sh, 1434m, 1386s, 1318m-sh (ν_{NO_3}) 1278s, 1244s-sh, 1212m-sh, 1157s, 1122s, 1094m, 1028m, 994m, 971m, 847w, 815m, 745m, 693s. Λ_m (MeOH, 1.1×10^{-3} M): $80 \text{ S cm}^{-2} \text{ mol}^{-1}$. UV/Vis (MeOH, 2.3×10^{-4} M): λ/nm ($\epsilon / \text{M}^{-1} \text{ cm}^{-1}$) = 260sh (2.2×10^4), 408 (3.0×10^4), 450 (2.7×10^4), 478 (2.2×10^4). ^1H NMR (CD_3OD): δ / ppm = 7.62–7.46 (m, 15H, Ph), 7.31 (d, $^3J_{\text{HH}} = 15.7$ Hz, 2H, C15-H), 7.12 (s, 2H, C22-H), 7.02 (d, $^3J_{\text{HH}} = 8.1$ Hz, 2H, C17-H), 6.82 (d, $^3J_{\text{HH}} = 8.1$ Hz, 2H, C18-H), 6.36 (d, $^3J_{\text{HH}} = 15.5$ Hz, 2H, C14-H), 5.79 (d, $^3J_{\text{HH}} = 6.1$ Hz, 2H, C4-H), 5.49 (d, $^3J_{\text{HH}} = 5.6$ Hz, 2H, C3-H), 5.31 (s, 1H, C12-H), 3.92 (s, 6H, C21-H), 2.67 (hept, $^3J_{\text{HH}} = 7.0$ Hz, 1H, C6-H), 1.97 (s, 3H, C1-H), 1.27 (d, $^3J_{\text{HH}} = 6.9$ Hz, 6H, C7-H). No change in the ^1H NMR spectrum was observed after 14 h at room temperature. $^{13}\text{C}\{^1\text{H}\}$ NMR (CD_3OD): δ / ppm = 181.3 (C13), 150.3 (C19), 149.5 (C20), 141.4 (C15), 135.5 (d, $^2J_{\text{CP}} = 10$ Hz, C9), 132.4 (d, $^4J_{\text{CP}} = 2$ Hz, C11), 131.2 (d, $^1J_{\text{CP}} = 46$ Hz, C8), 129.8 (d, $^3J_{\text{CP}} = 10$ Hz, C10), 128.9 (C16), 125.0 (C14), 124.1 (C17), 116.6 (C18), 111.5 (d, $^2J_{\text{CP}} = 4$ Hz, C5), 111.2 (C22), 106.0 (C12), 100.5 (C2), 90.1 (d, $^2J_{\text{CP}} = 4$ Hz, C4), 89.0 (d, $^2J_{\text{CP}} = 3$ Hz, C3), 56.5 (C21), 32.0 (C6), 22.4 (C7), 17.7 (C1). ^{14}N NMR (CD_3OD): δ / ppm = -3.5 ($\Delta\nu_{1/2} = 30$ Hz, NO_3^-). $^{31}\text{P}\{^1\text{H}\}$ NMR (CD_3OD): δ / ppm = 32.5. ^1H NMR (CDCl_3): δ / ppm = 7.56–7.38 (m, 15H, Ph), 7.29 (d, $^3J_{\text{HH}} = 15.6$ Hz, 2H, C15-H), 7.13 (d, $^4J_{\text{HH}} = 1.3$ Hz, 2H, C22-H), 7.01 (dd, $^3J_{\text{HH}} = 8.2$ Hz, $^4J_{\text{HH}} = 1.3$ Hz, 2H, C17-H), 6.93 (d, $^3J_{\text{HH}} = 8.2$ Hz, 2H, C18-H), 6.30 (s-br, 2H, OH), 6.18 (d, $^3J_{\text{HH}} = 15.6$ Hz, 2H, C14-H), 5.72 (d, $^3J_{\text{HH}} = 6.1$ Hz, 2H, C4-H), 5.39 (d, $^3J_{\text{HH}} = 6.0$ Hz, 2H, C3-H), 5.13 (s, 1H, C12-H), 4.00 (s, 6H, C21-H), 2.65 (hept, $^3J_{\text{HH}} = 6.6$ Hz, 1H, C6-H), 1.90 (s, 3H, C1-H), 1.21 (d, $^3J_{\text{HH}} = 6.2$ Hz, 6H, C7-H). $^{31}\text{P}\{^1\text{H}\}$ NMR (CDCl_3): δ / ppm = 33.5.

3. Study of the stability in solution

In DMSO/water. *General procedure.* A stock $[\text{D}_6]\text{DMSO}/\text{D}_2\text{O} = 7:3$ v/v solution containing dimethyl sulfone (Me_2SO , 6.4×10^{-3} M) as a reference for ^1H NMR spectra^[67] (δ / ppm = 2.95; s, 6H) in $[\text{D}_6]\text{DMSO}/\text{D}_2\text{O} = 7:3$ was used for the stability experiments. A freshly prepared solution of the selected Ru compound in the $[\text{D}_6]\text{DMSO}/\text{D}_2\text{O}$ mixture (0.6 mL, 1.2×10^{-2} M) was analyzed by ^1H and $^{31}\text{P}\{^1\text{H}\}$ NMR. Therefore the solution was maintained at 37 °C for 72 hours and periodically analysed by ^1H and $^{31}\text{P}\{^1\text{H}\}$ NMR upon brief cooling to room temperature. After 72 hours, $^{13}\text{C}\{^1\text{H}\}$ and ^{35}Cl NMR spectra were also recorded for **2** and **Ru-curc**, respectively. A parallel experiment was conducted with a $\text{DMSO}:\text{H}_2\text{O}$ 7:3 v/v solution of the selected Ru compound (4.0 mL, 1.2×10^{-3} M) for conductivity measurements. Results for each compound tested are reported in the Supporting Information (Tables S3–S6, Schemes S4–S7). The identity of compounds detected in solution was checked by comparison with NMR data of pure compounds (see NMR reference data in the SI). The (%) relative amount of compounds in solution were calculated by ^1H NMR integration and refer to identified compounds only (indicated as “% NMR”) or refer to Me_2SO_2 used as internal standard (indicated as “% NMR vs. internal standard”). Molar conductivity (Λ_m) was calculated with reference to the starting material.

In DMSO/cell culture medium. *General procedure.* The selected Ru compound (**2** or **[3]NO₃**) was dissolved in DMSO then diluted with RPMI 1640 cell culture medium. The resulting solution ($c_{\text{Ru}} = 1.8 \times 10^{-3}$ M) was maintained at 37 °C for 72 hours and periodically sampled for $^{31}\text{P}\{^1\text{H}\}$ NMR analysis (sealed C_6D_6 capillary for locking). Besides phosphate, only one signal was detected in the $^{31}\text{P}\{^1\text{H}\}$ NMR spectrum for the freshly prepared solution. After 72 hours, the solution was diluted with H_2O (15 mL) then extracted with CH_2Cl_2 (3x10 mL). The combined extracts were dried under vacuum (40 °C) and the resulting solid was analyzed by ^1H and $^{31}\text{P}\{^1\text{H}\}$ NMR (CD_3OD). Results are reported in the SI.

4. Interaction with Avidin

Relative affinity toward avidin was determined using Biotective™ Green reagent as described elsewhere.^[16b,18] Briefly, at least three independent stock solutions of the biotinylated compounds were prepared in DMSO and then a series of dilutions in phosphate-buffered saline were made. A total of 50 μL aliquots were transferred into wells of a 96-well black PP plate (Nunc brand, Thermo Fisher Scientific Inc., Waltham, MA USA) and 50 μL of Biotective™ Green reagent solution was added. The mixture was incubated in the dark for 15 min at room temperature and the fluorescence was measured in EnVision 2104 microplate reader (Perkin Elmer, Waltham, MA USA) using a 492/8 filter for excitation and a 530/10 for emission. The fluorescence intensity was proportional to the amount of biotinylated compound bound to avidin and this was plotted against the concentration of the test compound in GraphPad Prism 5.02 software (GraphPad Inc.). The apparent equilibrium dissociation constant, as a measure of the affinity, and the Hill coefficient, as a measure of the cooperativity between biotin-binding sites of an avidin molecule, were determined from these plots using equation:

$$B = (B_{\text{max}} \times \text{CH}) / (K_d + \text{CH})$$

where B is the amount of bound compound, B_{max} is maximum amount of bound compound, C is the compound concentration, H is the Hill coefficient and K_d is the apparent equilibrium dissociation constant.

5. Cytotoxicity Studies

A) Human ovarian carcinoma (A2780 and A2780cisR) cell lines were obtained from the European Collection of Cell Cultures. Penicillin streptomycin, RPMI 1640 GlutaMAX (where RPMI = Roswell Park Memorial Institute) were obtained from Life Technologies, and fetal bovine serum (FBS) was obtained from Sigma. The cells were cultured in RPMI 1640 GlutaMAX medium containing 10 % heat-inactivated FBS and 1 % penicillin streptomycin at 37 °C and CO_2 (5 %). The A2780cisR cell line was routinely treated with cisplatin (2 μM) in the media to maintain cisplatin resistance. The cytotoxicity was determined using the 3-(4,5-dimethyl 2-thiazolyl)-2,5-diphenyl-2H-tetrazolium bromide (MTT) assay.^[68] Cells were seeded in flat-bottomed 96-well plates as a suspension in a prepared medium (100 μL aliquots and approximately 4300 cells/well) and preincubated for 24 h. Stock solutions of compounds were prepared in DMSO and were diluted in medium. The solutions were sequentially diluted to give a final DMSO concentration of 0.5 % and a final compound concentration range (0–200 μM). Cisplatin and RAPTA-C were tested as a positive (0–100 μM) and negative (200 μM) controls respectively. The compounds were added to the preincubated 96-well plates in 100 μL aliquots, and the plates were incubated for a further 72 hours. MTT (20 μL , 5 mg/mL in Dulbecco's phosphate buffered saline) was added to the cells, and the plates were incubated for a further 4 h. The culture medium was aspirated and the purple formazan crystals, formed by the mitochondrial dehydrogenase activity of vital cells, were dissolved in DMSO (100 μL /well). The absorbance of the resulting solutions, directly proportional to the number of surviving cells, was quantified at 590 nm using a SpectroMax M5e multimode microplate reader (using SoftMax Pro software, version 6.2.2). The percentage of surviving cells was calculated from the absorbance of wells corresponding to the untreated control cells. The reported IC_{50} values are based on the means from two independent experiments, each comprising four tests per concentration level.

B) K562 (chronic myelogenous leukaemia), COLO 205, SW620 (human colorectal adenocarcinoma) and HCT 116 (human colorectal

carcinoma) cell lines were purchased from American Type Culture Collection (Manassas, VA USA). The cell lines were cultured in standard cell culture conditions (37 °C, 5 % CO₂, 95 % relative humidity) in high-glucose Dulbecco's Modified Eagle Medium (DMEM) buffered with HEPES and/or RPMI 1640 medium, supplemented with Glutamax-I and 10 % v/v foetal bovine serum (Thermo Fisher Scientific Inc., Waltham, MA USA). Care was taken to avoid cross-contamination between the cell lines. The cells were tested every 3 months for *Mycoplasma* contamination with a MycoProbe[®] Mycoplasma Detection Kit by R&D (Minneapolis, MN USA).

Cell viability was determined by a modified MTT reduction assay.^[69] Cells suspended in 100 µL of a complete medium were seeded on 96-well plates at a density of 104/well. The cells were allowed to attach for about 24 hours and then the investigated substance was added at the desired concentration in the range between 3 nM and 30 µM. Stock solutions were prepared in DMSO and the solvent concentration was maintained constant in all wells, including the controls. The final DMSO concentration did not exceed 0.1 % v/v and was determined to be non-toxic to the cells. After 70 hours of incubation, MTT was added to the medium to a final concentration of 1.1 mM. After additional 2 hours, the medium was removed and the formazan crystals were dissolved in 100 µL of DMSO. The absorbance was measured at 580 nm analytic wavelength and 720 nm reference wavelength in EnVision 2104 microplate reader (Perkin Elmer, Waltham, MA USA). The results were turned into percentage of controls and the IC₅₀ values for each cell line and substance were calculated with the GraphPad Prism 5.02 software (GraphPad Inc.) using a four-parameter nonlinear logistic regression.

6. Cell Lysate Preparation and Protein Content Determination

Following aspiration of the culture medium, cells were washed with ice-cold phosphate-buffered saline (PBS) and then scraped off the flask surface and suspended in 1 mL of PBS. Then, the cells were transferred to 15-mL tubes and centrifuged (100 × g, 10 min, 4°C). Supernatant was aspirated and cells were washed in PBS again. Finally, the cells were suspended in 0.1 % SDS solution enriched with Halt[™] Protease Inhibitor Cocktail (Thermo Fisher Scientific Inc., Waltham, MA USA) and kept in -20°C overnight. Protein content was determined by a modified Lowry assay^[70] (original tartrate replaced by citrate) using bovine serum albumin as a protein standard. Absorbance was measured at 750 nm in EnVision 2104 microplate reader (Perkin Elmer, Waltham, MA USA). Sample protein content was calculated from the standard curve.

7. SDS-PAGE and Western Blotting

The cell lysate samples (20 µg of protein) were subjected to SDS-polyacrylamide gel electrophoresis in gradient gels according to Laemmli.^[71] Tris/glycine/SDS running buffer was used. Electrophoresis was performed at 140 V until adequate separation of the molecular weight markers was achieved. Then, the proteins were transferred onto Trans-Blot Turbo Mini Format polyvinylidene difluoride (PVDF) membrane using a semi-dry transfer system (Bio-Rad, Richmond, CA USA). Anti-SMVT antibody was used at a dilution of 1:400, anti-β-actin antibody was used at a dilution of 1:2,000. Proteins of interest were identified using horseradish peroxidase-labelled anti-mouse antibody at a dilution 1:2,000 for both primary antibodies. The blots were then developed by an enhanced chemiluminescence detection system. The relative intensity of the bands was quantified by scanning densitometry analysis using the NIH Image application of Uvitec Cambridge Alliance[®] HD4 Mini imaging system (Cleaver Scientific Ltd, Rugby, Warwickshire, UK).

Supporting Information (see footnote on the first page of this article): Spectroscopic data and IR, NMR and UV/Vis spectra of compounds; details of stability studies.

Acknowledgments

We thank the University of Pisa (PRA 2017: “*Composti di metalli di transizione come possibili agenti antitumorali*”), the University of Łódź and the Swiss National Science Foundation for financial support.

Keywords: Ruthenium · Phosphine ligands · Arene complexes · Biotin · Cytotoxicity

- [1] a) R. G. Kenny, C. J. Marmion, *Chem. Rev.* **2019**, *119*, 1058–1137; b) P. Zhang, P. J. Sadler, *J. Organomet. Chem.* **2017**, *839*, 5–14; c) C. S. Al-lardyce, P. J. Dyson, *Dalton Trans.* **2016**, *45*, 3201–3209.
- [2] a) E. Alessio, *Eur. J. Inorg. Chem.* **2017**, 1549–1560; b) S. M. Meier-Menches, C. Gerner, W. Berger, C. G. Hartinger, B. K. Keppler, *Chem. Soc. Rev.* **2018**, *47*, 909–928, and references cited therein.
- [3] I. Bratsos, T. Gianferrara, E. Alessio, C. G. Hartinger, M. A. Jakupec, B. K. Keppler, in *Bioinorganic Medicinal Chemistry* (Ed.: E. Alessio), Wiley-VCH, Weinheim **2011**, pp. 151–174.
- [4] a) A. Pettenuzzo, D. Montagner, P. McArdle, L. Ronconi, *Dalton Trans.* **2018**, *47*, 10721–10736; b) L. N. Lameijer, S. L. Hopkins, T. G. Brevé, S. H. C. Askes, S. Bonnet, *Chem. Eur. J.* **2016**, *22*, 18484–18491; c) M. Patra, T. C. Johnstone, K. Suntharalingam, S. J. Lippard, *Angew. Chem. Int. Ed.* **2016**, *55*, 2550–2554; *Angew. Chem.* **2016**, *128*, 2596; d) J. P. Parker, M. Devocelle, M. P. Morgan, C. J. Marmion, *Dalton Trans.* **2016**, *45*, 13038–13041; e) A. M. McKeon, J. Noonan, M. Devocelle, B. M. Murphy, D. M. Griffith, *Chem. Commun.* **2017**, *53*, 11318–11321.
- [5] C. M. Paulos, M. J. Turk, G. J. Breur, P. S. Low, *Adv. Drug Delivery Rev.* **2004**, *56*, 1205–1217.
- [6] L. M. Bareford, B. R. Avaritt, H. Ghandehari, A. Nan, P. W. Swaan, *Pharm. Res.* **2013**, *30*, 1799–1812.
- [7] a) B. R. Schroeder, M. I. Ghare, C. Bhattacharya, R. Paul, Z. Yu, P. A. Zaleski, T. C. Bozeman, M. J. Rishel, S. M. Hecht, *J. Am. Chem. Soc.* **2014**, *136*, 13641–13656; b) M. Potter, E. Newport, K. J. Morten, *Biochem. Soc. Trans.* **2016**, *44*, 1499–1505; c) See ref.^[4a] d) A. Berger, M. Hanif, A. A. Nazarov, C. G. Hartinger, R. John, M. L. Kuznetsov, M. Groessl, F. Schmitt, O. Zava, F. Biba, V. B. Arion, M. Galanski, M. A. Jakupec, L. Juillierat-Jeanerret, P. J. Dyson, K. Keppler, *Chem. Eur. J.* **2008**, *14*, 9046–9057; e) M. Hanif, A. A. Nazarov, C. G. Hartinger, W. Kandlioller, M. A. Jakupec, V. B. Arion, P. J. Dyson, B. K. Keppler, *Dalton Trans.* **2010**, *39*, 7345–7352.
- [8] a) J.-F. Shi, P. Wu, Z.-H. Jiang, X.-Y. Wei, *Eur. J. Med. Chem.* **2014**, *71*, 219–228; b) J. Zhao, W. Hua, G. Xu, S. Gou, *J. Inorg. Biochem.* **2017**, *176*, 175–180.
- [9] Selected recent references include: a) J. Luo, X. Meng, J. Su, H. Ma, W. Wang, L. Fang, H. Zheng, Y. Qin, T. Chen, *J. Agric. Food Chem.* **2018**, *66*, 9219–9230; b) N. U. Deshpande, M. Jayakannan, *Biomacromolecules* **2018**, *19*, 3572–3585; c) Y. Singh, K. K. Durga Rao Viswanadham, A. Kumar Jajoriya, J. Gopal Meher, K. Raval, S. Jaiswal, J. Dewangan, H. K. Bora, S. Kumar Rath, J. Lal, D. Prasad Mishra, M. K. Chourasia, *Mol. Pharm.* **2017**, *14*, 2749–2765; d) Ł. Uram, M. Szuster, A. Filipowicz, M. Zare, E. Walajtys-Rode, S. Wołowicz, *Bioorg. Med. Chem.* **2017**, *25*, 706–713; e) N. Nateghian, N. Goodarzi, M. Amini, F. Atyabi, M. Reza Khorramizadeh, R. Dinarvand, *Chem. Biol. Drug Des.* **2016**, *87*, 69–82; f) L. Cao, G. Hettiarachchi, V. Briken, L. Isaacs, *Angew. Chem. Int. Ed.* **2013**, *52*, 12033–12037; *Angew. Chem.* **2013**, *125*, 12255.
- [10] a) Y. Yamazaki, K. Kohno, H. Yasui, Y. Kiso, M. Akamatsu, B. Nicholson, G. Deyanat-Yazdi, S. Neuteboom, B. Potts, G. Kenneth Lloyd, Y. Hayashi, *ChemBioChem* **2008**, *9*, 3074–3081; b) S. Maiti, N. Park, J. Hye Han, H. Mi Jeon, J. Hong Lee, S. Bhuniya, C. Kang, J. Seung Kim, *J. Am. Chem. Soc.* **2013**, *135*, 4567–457; c) Y. Venkatesh, S. Karthik, Y. Rajesh, M. Mandal, A. Jana, N. D. Pradeep Singh, *Chem. Asian J.* **2016**, *11*, 3482–3486.
- [11] a) K. Kam-Wing Lo, M.-W. Louie, K.-S. Sze, J. Shing-Yip Lau, *Inorg. Chem.* **2008**, *47*, 602–611; b) Z. Zhao, P. Gao, Y. You, T. Chen, *Chem. Eur. J.* **2018**, *24*, 3289–3298; c) B. Siewert, M. Langerman, A. Pannwitz, S. Bonnet, *Eur. J. Inorg. Chem.* **2018**, 4117–4124; d) L. Corte-Real, B. Karas, P. Girio, A. Moreno, F. AVECILLA, F. Marques, B. T. Buckley, K. R. Cooper, C. Doherty, P. Falson, M. H. Garcia, A. Valente, *Eur. J. Med. Chem.* **2019**, *163*, 853–863;

- e) A. Kumar, S. Daya, S. Pandey, Q. Xua, P. Braunstein, *Coord. Chem. Rev.* **2014**, 270–271, 31–56.
- [12] X. Li, C.-y. Kim, S. Lee, D. Lee, H.-M. Chung, G. Kim, S.-H. Heo, C. Kim, K.-S. Hong, J. Yoon, *J. Am. Chem. Soc.* **2017**, 139, 10880–10886.
- [13] B. Bertrand, M. A. O'Connell, Z. A. E. Waller, M. Bochmann, *Chem. Eur. J.* **2018**, 24, 3613–3622.
- [14] a) K. Mitra, A. Shettar, P. Kondaiah, A. R. Chakravarty, *Inorg. Chem.* **2016**, 55, 5612–5622; b) J. Hu, T.-M. Wu, H.-Z. Li, Z.-P. Zuo, Y.-L. Zhao, L. Yang, *Bioorg. Med. Chem. Lett.* **2017**, 27, 3591–3594.
- [15] N. Muhammad, N. Sadia, C. Zhu, C. Luo, Z. Guo, X. Wang, *Chem. Commun.* **2017**, 53, 9971–9974.
- [16] a) D. Plazuk, J. Zakrzewski, M. Salmain, A. Błauz, B. Rychlik, P. Strzelczyk, A. Bujacz, G. Bujacz, *Organometallics* **2013**, 32, 5774–5783; b) A. Błauz, B. Rychlik, A. Makal, K. Szulc, P. Strzelczyk, G. Bujacz, J. Zakrzewski, K. Wozniak, D. Plazuk, *ChemPlusChem* **2016**, 81, 1191–1201.
- [17] S. M. Meier, D. Kreutz, L. Winter, M. H. M. Klose, K. Cseh, T. Weiss, A. Bileck, B. Alte, J. C. Mader, S. Jana, A. Chatterjee, A. Bhattacharyya, M. Hejl, M. A. Jakupc, P. Heffeter, W. Berger, C. G. Hartinger, B. K. Keppler, G. Wiche, C. Gerner, *Angew. Chem. Int. Ed.* **2017**, 56, 8267–8271; *Angew. Chem.* **2017**, 129, 8379.
- [18] M. V. Babak, D. Plazuk, S. M. Meier, H. J. Arabshahi, J. Reynisson, B. Rychlik, A. Błauz, K. Szulc, M. Hanif, S. Strobl, A. Roller, B. K. Keppler, C. G. Hartinger, *Chem. Eur. J.* **2015**, 21, 5110–5117.
- [19] G. Agonigi, T. Riedel, S. Zacchini, E. Păunescu, G. Pampaloni, N. Bartalucci, P. J. Dyson, F. Marchetti, *Inorg. Chem.* **2015**, 54, 6504–6512.
- [20] a) L. Biancalana, S. Zacchini, N. Ferri, M. G. Lupo, G. Pampaloni, F. Marchetti, *Dalton Trans.* **2017**, 46, 16589–16604; b) L. Biancalana, G. Pampaloni, F. Marchetti, *Chimia* **2017**, 71, 573–579.
- [21] a) L. Biancalana, L. K. Batchelor, A. De Palo, S. Zacchini, G. Pampaloni, P. J. Dyson, F. Marchetti, *Dalton Trans.* **2017**, 46, 12001–12004; b) L. Biancalana, A. Pratesi, F. Chiellini, S. Zacchini, T. Funaioli, C. Gabbiani, F. Marchetti, *New J. Chem.* **2017**, 41, 14574–14588.
- [22] B. Neises, W. Steglich, *Angew. Chem. Int. Ed. Engl.* **1978**, 17, 522–524; *Angew. Chem.* **1978**, 90, 556.
- [23] K. M. Nelson, J. L. Dahlin, J. Bisson, J. Graham, G. F. Pauli, M. A. Walters, *J. Med. Chem.* **2017**, 60, 1620–1637.
- [24] a) F. Kiihlwein, K. Polborn, W. Beck, Z. *Anorg. Allg. Chem.* **1997**, 623, 1211–1219; b) F. Caruso, M. Rossi, A. Benson, C. Opazo, D. Freedman, E. Monti, M. B. Gariboldi, J. Shaulyk, F. Marchetti, R. Pettinari, C. Pettinari, *J. Med. Chem.* **2012**, 55, 1072–1081.
- [25] a) R. Pettinari, F. Marchetti, F. Condello, C. Pettinari, G. Lupidi, R. Scopelliti, S. Mukhopadhyay, T. Riedel, P. J. Dyson, *Organometallics* **2014**, 33, 3709–3715; b) R. Pettinari, F. Condello, F. Marchetti, C. Pettinari, P. Smoleński, T. Riedel, R. Scopelliti, P. J. Dyson, *Eur. J. Inorg. Chem.* **2017**, 2905–2910.
- [26] Despite the Ru atom in **1** and **2** is not chiral, non equivalence of the Ru-CH groups of the η^6 -arene ligand (C3, C4 in Scheme 3 and Scheme 4) and, to a less extent, of the PPh₂ groups (C8–C11 in Scheme 3 and Scheme 4) is observed in ¹H and ¹³C NMR spectra. Such atoms/groups are diastereotopic due to the presence of the biotinyl group. This effect is not appreciable in the NMR spectra of [3]NO₃.
- [27] a) L. Biancalana, G. Ciancaleoni, S. Zacchini, A. Monti, F. Marchetti, G. Pampaloni, *Organometallics* **2018**, 37, 1381–1391, and references cited therein; b) G. Ludwig, G. N. Kaluderović, M. Bette, M. Block, R. Paschke, D. Steinborn, *J. Inorg. Biochem.* **2012**, 113, 77–82; c) O. Kühn, *Phosphorus-31 NMR Spectroscopy*, **2008**, Springer-Verlag Berlin Heidelberg.
- [28] a) H. Yan, G. Süß-Fink, A. Neels, H. Stoeckli-Evans, *J. Chem. Soc., Dalton Trans.* **1997**, 4345–4350; b) W. H. Ang, E. Daldini, C. Scolari, R. Scopelliti, L. Juillerat-Jeannerat, P. J. Dyson, *Inorg. Chem.* **2006**, 45, 9006–9013.
- [29] R. E. Goldbach, I. Rodriguez-Garcia, J. H. van Lenthe, M. A. Siegler, S. Bonnet, *Chem. Eur. J.* **2011**, 17, 9924–9929.
- [30] a) B. Demerseman, R. Le Lagadec, B. Guilbert, C. Renouard, P. Crochet, P. H. Dixneuf, *Organometallics* **1994**, 13, 2269–2283; b) M. Gaye, B. Demerseman, P. H. Dixneuf, *J. Organomet. Chem.* **1992**, 424, 65–70; c) M. Gaye, B. Demerseman, P. H. Dixneuf, *J. Organomet. Chem.* **1991**, 411, 263–270; d) B. Demerseman, C. Renouard, R. Le Lagadec, M. Gonzalez, P. Crochet, P. H. Dixneuf, *J. Organomet. Chem.* **1994**, 471, 229–239.
- [31] Analogous chemical shift variations were observed for CDCl₃ and [D₆]-acetone solutions of [RuCl(cucr)(η^6 -p-cymene)] (**Ru-cucr**). According to molar conductivity data,^[24b] **Ru-cucr** exists in chlorinated solvents whereas ionization to the solvato-species [Ru(cucr)(η^6 -p-cymene)(acetone)]⁺ occurs in acetone.
- [32] N. Logan, Applications of ¹⁴N NMR Data in the Study of Inorganic Molecules. In: (Eds.: M. Witanowski, G. A. Webb), *Nitrogen NMR*, **1973**, Springer, Boston, MA.
- [33] ¹⁴N NMR data for NaNO₃: ¹⁴N NMR (D₂O): δ /ppm = –5.0 ($\Delta\nu_{1/2}$ = 7 Hz); ¹⁴N NMR (CH₃OD): δ /ppm = –2.7 ($\Delta\nu_{1/2}$ = 14 Hz).
- [34] F. A. Miller, C. H. Wilkins, *Anal. Chem.* **1952**, 24, 1253–1294.
- [35] A. Levina, D. C. Crans, P. A. Lay, *Coord. Chem. Rev.* **2017**, 352, 473–498.
- [36] C. Lipinski, Drug Solubility in Water and Dimethyl sulfoxide. In *Molecular Drug Properties* (Eds.: R. Mannhold, H. Kubinyi, G. Folkers, R. Mannhold), Wiley Ed., **2008**.
- [37] a) I. Bratsos; E. Alessio, *Inorg. Synth.* **2010**, 35, 148–152; b) E. Alessio, *Chem. Rev.* **2004**, 104, 4203–4242.
- [38] a) A. B. Chaplin, P. J. Dyson, *J. Organomet. Chem.* **2011**, 696, 2485–2490; b) F. Aman, M. Hanif, W. Ahmad Siddiqui, A. Ashraf, L. K. Filak, J. Reynisson, T. Söhnel, S. M. F. Jamieson, C. G. Hartinger, *Organometallics* **2014**, 33, 5546–5553; c) M. V. Babak, S. M. Meier, K. V. M. Huber, J. Reynisson, A. A. Legin, M. A. Jakupc, A. Roller, A. Stukalov, M. Gridling, K. L. Bennett, J. Colinge, W. Berger, P. J. Dyson, G. Superti-Furga, B. K. Keppler, C. G. Hartinger, *Chem. Sci.* **2015**, 6, 2449–2456; d) S. Movassaghi, E. Leung, M. Hanif, B. Y. T. Lee, H. U. Holtkamp, J. K. Y. Tu, T. Söhnel, S. M. F. Jamieson, C. G. Hartinger, *Inorg. Chem.* **2018**, 57, 8521–8529.
- [39] H. Charvatov, T. Riedel, I. Cisarova, P. J. Dyson, P. Stepnicka, *J. Organomet. Chem.* **2016**, 802, 21–26.
- [40] a) M. Patra, T. Joshi, V. Pierroz, K. Ingram, M. Kaiser, S. Ferrari, B. Spingler, J. Keiser, G. Gasser, *Chem. Eur. J.* **2013**, 19, 14768–14772; b) J. Kljun, A. J. Scott, T. Lanisnik Rizner, J. Keiser, I. Turel, *Organometallics* **2014**, 33, 1594–1601; c) S. Moon, M. Hanif, M. Kubanik, H. Holtkamp, T. Söhnel, S. M. F. Jamieson, C. G. Hartinger, *ChemPlusChem* **2015**, 80, 231–236; d) E. Paunescu, S. McArthur, M. Soudani, R. Scopelliti, P. J. Dyson, *Inorg. Chem.* **2016**, 55, 1788–1808.
- [41] a) P. Mandal, B. Kumar Kundu, K. Vyas, V. Sabu, A. Helen, S. Singh Dhankhar, C. M. Nagaraja, D. Bhattacherjee, K. Pada Bhabake, S. Mukhopadhyay, *Dalton Trans.* **2018**, 47, 517–527; b) L. Biancalana, G. Pampaloni, S. Zacchini, F. Marchetti, *J. Organomet. Chem.* **2018**, 869, 201–211.
- [42] L. Biancalana, G. Pampaloni, S. Zacchini, F. Marchetti, *J. Organomet. Chem.* **2017**, 848, 214–221. <lit43K. J. Kilpin, S. M. Cammack, C. M. Clavel, P. J. Dyson, *Dalton Trans.* **2013**, 42, 2008.
- [44] S. Parveen, M. Hanif, S. Movassaghi, M. P. Sullivan, M. Kubanik, M. Ashraf Shaheen, T. Söhnel, S. M. F. Jamieson, C. G. Hartinger, *Eur. J. Inorg. Chem.* **2017**, 1721–1727.
- [45] S. Tasan, O. Zava, B. Bertrand, C. Bernhard, C. Goze, M. Picquet, P. Le Gendre, P. Harvey, F. Denat, A. Casini, E. Bodio, *Dalton Trans.* **2013**, 42, 6102–6109.
- [46] a) T. Gianferrara, I. Bratsos, E. Alessio, *Dalton Trans.* **2009**, 7588–7598; b) Z. Adhiksekan, G. E. Davey, P. Campomanes, M. Groessl, C. M. Clavel, H. Yu, A. A. Nazarov, C. Hui Fang Yeo, W. Han Ang, P. Dröge, U. Rothlisberger, P. J. Dyson, C. A. Davey, *Nat. Commun.* **2014**, 5, Article number: 3462; c) W. Han Ang, L. J. Parker, A. De Luca, L. Juillerat-Jeanneret, C. J. Morton, M. Lo Bello, M. W. Parker, P. J. Dyson, *Angew. Chem. Int. Ed.* **2009**, 48, 3854–3857; *Angew. Chem.* **2009**, 121, 3912.
- [47] a) A. Bergamo, A. Masi, A. F. A. Peacock, A. Habtemariam, P. J. Sadler, G. Sava, *J. Inorg. Biochem.* **2010**, 104, 79–86 and references cited therein; b) R. H. Berndsen, A. Weiss, U. Kulsoom Abdul, T. J. Wong, P. Meraldi, A. W. Griffioen, P. J. Dyson, P. Nowak-Sliwinska, *Sci. Rep.* **2017**, 7, 43005 and references cited therein.
- [48] a) C. Scolari, C. G. Hartinger, C. S. Allardyce, B. K. Keppler, P. J. Dyson, *J. Inorg. Biochem.* **2008**, 102, 1743–1748; b) F. Wang, H. Chen, S. Parsons, I. D. H. Oswald, J. E. Davidson, P. J. Sadler, *Chem. Eur. J.* **2003**, 9, 5810–5820.
- [49] a) M. Groessl, M. Terenghi, A. Casini, L. Elviri, R. Lobinski, P. J. Dyson, *J. Anal. At. Spectrom.* **2010**, 25, 305–313; b) W. Hu, Q. Luo, X. Ma, K. Wu, J. Liu, Y. Chen, S. Xiong, J. Wang, P. J. Sadler, F. Wang, *Chem. Eur. J.* **2009**, 15, 6586–6594; c) W. Guo, W. Zheng, Q. Luo, X. Li, Y. Zhao, S. Xiong, F. Wang, *Inorg. Chem.* **2013**, 52, 5328–5338.
- [50] a) C. G. Hartinger, A. Casini, C. Duhot, Y. O. Tsybin, L. Messori, P. J. Dyson, *J. Inorg. Biochem.* **2008**, 102, 2136–2141; b) F. Wang, J. Xu, A. Habtemariam, J. Bella, P. J. Sadler, *J. Am. Chem. Soc.* **2005**, 127, 17734–17743.

- [51] a) F. Wang, H. Chen, J. A. Parkinson, P. d. S. Murdoch, P. J. Sadler, *Inorg. Chem.* **2002**, *41*, 4509–4523; b) F. Wang, J. Bella, J. A. Parkinson, P. J. Sadler, *J. Inorg. Biochem.* **2005**, *10*, 147–155.
- [52] S. I. Lehtonen, A. Tullila, N. Agrawal, S. Kukkurainen, N. Kähkönen, M. Koskinen, T. K. Nevanen, M. S. Johnson, T. T. Airene, M. S. Kulomaa, T. A. Riihimäki, V. P. Hytönen, *ACS Chem. Biol.* **2016**, *11*, 211–221.
- [53] B. S. Murray, M. V. Babak, C. G. Hartinger, P. J. Dyson, *Coord. Chem. Rev.* **2016**, *306*, 86–114 and references cited therein.
- [54] C. Scolari, A. Bergamo, L. Brescacin, R. Delfino, M. Cocchietto, G. Laurency, T. J. Geldbach, G. Sava, P. J. Dyson, *J. Med. Chem.* **2005**, *48*, 4161–4171.
- [55] A. K. Renfrew, R. Scopelliti, P. J. Dyson, *Inorg. Chem.* **2010**, *49*, 2239–2246.
- [56] H. Baker, B. DeAngelis, O. Frank, *Experientia* **1988**, *44*, 1007–1010.
- [57] Fetal bovine serum used as an obligatory additive may contain some biotin, contributing to the final biotin composition.
- [58] A. Azhar, G. W. Booker, S. W. Polyak, *Biochem. Anal. Biochem.* **2015**, *4:4*, 1000210.
- [59] C. S. Allardyce, P. J. Dyson, D. J. Ellis, S. L. Heath, *Chem. Commun.* **2001**, 1396–1397.
- [60] a) M. A. Bennett, A. K. Smith, *J. Chem. Soc., Dalton Trans.* **1974**, 233–241; b) optimized procedure in ref. 41b.
- [61] G. R. Fulmer, A. J. M. Miller, N. H. Sherden, H. E. Gottlieb, A. Nudelman, B. M. Stoltz, J. E. Bercaw, K. I. Goldberg, *Organometallics* **2010**, *29*, 2176–2179.
- [62] R. K. Harris, E. D. Becker, S. M. Cabral De Menezes, R. Goodfellow, P. Granger, *Pure Appl. Chem.* **2001**, *73*, 1795–1818.
- [63] W. Willker, D. Leibfritz, R. Kerssebaum, W. Bermel, *Magn. Reson. Chem.* **1993**, *31*, 287–292.
- [64] F. Menges, “Spectragryph - optical spectroscopy software”, Version 1.2.9, @ **2018**, <http://www.ffmpeg2.de/spectragryph>.
- [65] a) A. Jutand, *Eur. J. Inorg. Chem.* **2003**, 2017–2040; b) W. J. Geary, *Coord. Chem. Rev.* **1971**, *7*, 81–122.
- [66] Molar conductivity data for reference compounds. NaNO₃. Λ_m (MeOH, 1.7–2.0 × 10⁻³ M): 119 S cm² mol⁻¹. NaCl. Λ_m (MeOH, 2.1–3.0 × 10⁻³ M) = 109 S cm² mol⁻¹.
- [67] T. Rundlöf, M. Mathiasson, S. Bekiroglu, B. Hakkarainen, T. Bowden, T. Arvidsson, *J. Pharm. Biomed. Anal.* **2010**, *52*, 645–651.
- [68] T. Mosmann, *J. Immunol. Methods* **1983**, *65*, 55–63.
- [69] J. Carmichael, W. DeGraff, A. Gazdar, J. Minna, J. Mitchell, *Cancer Res.* **1987**, *47*, 936–942.
- [70] O. H. Lowry, N. J. Rosebrough, A. L. Farr, R. J. Randall, *J. Biol. Chem.* **1951**, *193*, 265–275.
- [71] U. K. Laemmli, *Nature* **1970**, *227*, 680–685.

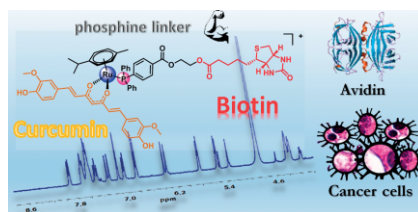
Received: August 27, 2019

Ruthenium-Biotin Conjugates

L. Biancalana, M. Gruchala,
L. K. Batchelor, A. Błauż, A. Monti,
G. Pampaloni, B. Rychlik,
P. J. Dyson, F. Marchetti* 1–13



Conjugating Biotin to Ruthenium(II) Arene Units via Phosphine Ligand Functionalization



Robust ruthenium(II) arene compounds incorporating biotin through a phosphine linkage were synthesized and assessed for their cytotoxicity against several cancer cell lines with different levels of biotin transporter expression, and for their apparent affinity to avidin.

DOI: 10.1002/ejic.201900922